Hindawi
Mathematical Problems in Engineering
Volume 2024, Article ID 5570228, 21 pages
https://doi.org/10.1155/2024/5570228

*Research Article*

# Chaotic Wind-Driven Optimization with Hyperbolic Tangent Model and *T*-Distributed Mutation Strategy

**Da Fang**,[1] **Jun Yan**,[1] **and Quan Zhou**[2]

[1]*Wuhan Technical College of Communications, Wuhan 430065, China*
[2]*Hubei Communications Technical College, Wuhan 430079, China*

Correspondence should be addressed to Da Fang; henrytoto@126.com

Received 13 June 2023; Revised 4 November 2023; Accepted 16 December 2023; Published 29 January 2024

Academic Editor: Taoreed Owolabi



Meta-heuristic algorithms have the advantages of resilience, global optimization capacity, and coding flexibility, making them helpful in tackling difficult optimization issues. The enhanced wind-driven optimization (CHTWDO) that was proposed in this paper coupled the chaotic map approach and the hyperbolic tangent with the *T*-distribution mutation method. The initial air particles are evenly distributed in the system space through a tent mapping strategy. Meanwhile, the variation probability of the hyperbolic tangent model and the *T*-distribution variation method are used to improve the comprehensive performance of the algorithm. In this way, the global search accuracy and the ability of avoiding the extreme value of the algorithm can be taken into account. Combining the three strategies, CHTWDO had higher global search accuracy and a stronger ability to jump out of local extremum. Comparing with the eight meta-heuristic algorithms (including WDO) and the single strategy improved WDO on 24 test functions, the experimental results show that CHTWDO with two improved strategies has better convergence precision and faster convergence speed. Statistical tests such as Friedman's and Wilcoxon's rank-sum tests are used to determine significant differences between these comparison algorithms. Finally, CHTWDO also obtains the best results on four classical optimization problems in engineering applications, which verifies its practicality and effectiveness.

## 1. Introduction

Since the 21st century, searching for new algorithms that can solve multidimension, multiobjective, and multimode gradually becomes a direction in the field of scientific research [1]. Meta-heuristic algorithm has the advantages of intuition and wide applicability and has been widely concerned by many scholars. The meta-heuristic algorithm is developed on the basis of an optimization algorithm [2]. While the optimization algorithm can solve the exact optimal solution according to the planning, the meta-heuristic algorithm can obtain a feasible solution of the problem at an acceptable cost, and the degree of deviation between the feasible solution and the optimal solution is unknown [3].

The meta-heuristic algorithm mainly comes from four directions: (1) based on natural laws, such as genetic algorithm (GA) [4], virulence optimization algorithm [5]; (2) based on physical laws, for example, simulated annealing algorithms [6], heat transfer search [7]; (3) human behavior, such as teaching-learning-based optimization [8], fireworks algorithm [9]; and (4) group-based ideas, such as particle swarm optimization (PSO) [10], whale optimization algorithm (WOA) [11], salp swarm algorithm [12], gray wolf optimizer (GWO) [13], ant colony algorithm [14], butterfly optimization algorithm [15], etc. These four directions belong to the group-based metaheuristic algorithm, which has the most achievements and is the most widely used. However, according to the NFL (no free lunch) theorem, in reality, there is no algorithm that can have a good effect on all problems [16]. Therefore, it is necessary to study new meta-heuristic algorithms and improve existing ones [17–19].

Dr. Bayraktar Z, Werner D H and Komurcu M, Penn State University, USA, at IEEE Antennas and Propagation Society International Symposium in 2010 Wind Driven Optimization (WDO): "A novel nature-inspired optimization algorithm and its application to electromagnetic [20]."

The wind-driven optimization (WDO) algorithm is also a group-based meta-heuristic algorithm, which is realized by

simulating the force movement of a simplified air particle [21]. WDO provides the benefits of a straightforward structure, minimal parameters, and ease of programing. Since the method was first developed, a growing number of academics have paid notice, using it in several circumstances and improving it in a variety of ways.

In combination with Newton's second law and the ideal gas equation of state, the updated equation of air particle velocity and position can be obtained. The algorithm has the advantages of simple principle, easy implementation, adjustable parameters, and not easy to fall into the local extreme value, and the equation of the algorithm has practical physical significance. Sokolik [22], Lin and Lin [23], and Tang et al. [24] investigated WDO on benchmark functions and used it for the first time to create a double-sided artificial magnetic conducting surface. It just serves to demonstrate WDO's usefulness and efficacy. In literature [20], WDO was used to synthesize a stub-loaded inverted-F antenna. It shows how successfully WDO handles electromagnetic optimization issues. WDO was used in literature [25] to create high-impedance metasurfaces. It shows how effective WDO is at creating high-impedance metasurfaces. It was used to address three electromagnetic optimization issues as well as unimodal and multimodal functions [26]. The findings demonstrate that WDO is frequently superior to certain popular evolutionary algorithms in the field of electromagnetics. To sustain population variety, collision avoidance technology and the multi-region concept in meteorology were added into WDO in literature [27]. A novel multiregion and anticollision WDO variation was provided as a result, and the enhanced technique was then used to solve dynamic optimization issues. With the efforts of more and more researchers, more and more improvements have been incorporated into the wind-driven algorithm. A WDO (WDOLE) with lévy flights is proposed. It is verified that WDOLE outperforms WDO on the benchmark function. Literature [28] proposed an improved algorithm of hybrid WDO and differential evolution, which can find better solutions. In literature [29], an adaptive WDO algorithm (AWDO) was proposed. This algorithm mainly uses covariance matrix adaptive evolutionary strategy (CMAES) to update parameters. In literature [30], a Wind Driven Butterfly Optimization Algorithm (WDBO) was used proportional-integral-derivative (PID) controller parameter optimization. In addition to electromagnetic applications, a variety of WDO algorithms are gradually applied to other fields. In literature [31], WDO was used to solve the multiobjective optimization issue of switching reluctance motor design. WDO was used in literature [32] to estimate solar photovoltaic characteristics. The results from WDO show greater precision. In literature [33], AWDO based on Chenlo's model was used to derive the solar cell model's parameters. It is a trustworthy and effective technique. In literature [27], a wind-driven fusion cuckoo search optimizes the algorithm to solve hyperspectral band selection problems. It can be seen from the NFL theorem [34, 35] that it is unrealistic to solve all the most important problems through one algorithm, which prompts us to improve the WDO algorithm to better solve various optimization problems.

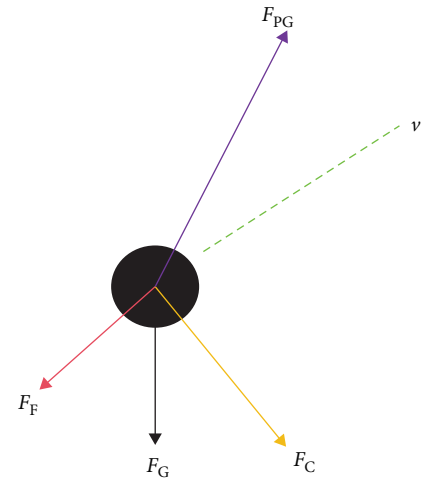


Figure 1: Proton force map in air.

## 2. WDO Algorithm

First, the air in the atmosphere is simplified into particles to deal with, here called air particles. According to Newton's second law in the noninertial coordinate system and the ideal gas equation of state, the model can be simplified, and the WDO algorithm can be obtained.

$$\rho\omega = \sum F_i, \tag{1}$$

where $\rho$ is the density of air particle; $\omega$ is acceleration; $F_i$ is the force exerted on the air particle. According to aerodynamics, there are four main forces applied to air as follows:

$$F_G = \rho\delta V g, \tag{2}$$

$$F_{PG} = -\nabla p\delta V, \tag{3}$$

$$F_C = -2\Omega \times u, \tag{4}$$

$$F_F = -\rho a u, \tag{5}$$

where $F_G$ is gravity; $F_{PG}$ is pressure gradient force; $F_C$ is Coriolis force; $F_F$ is the friction force; $\delta V$ is the volume of air particle; $g$ is the acceleration vector of gravity; $\nabla p$ is the pressure gradient (minus sign stands for going down along the gradient). $\Omega$ is the earth rotation angle vector; $u$ is wind velocity vector; $a$ is the friction coefficient. Figure 1 shows the proton force map in air.

By substituting Equations (2)–(5) and $\omega = \frac{\Delta u}{\Delta t}$ into Equation (1), we can get the following:

$$\rho\frac{\Delta u}{\Delta t} = \rho\delta V g - \nabla p\delta V - 2\Omega \times u - \rho a u. \tag{6}$$

In order to simplify the equation, let $\Delta t = 1$, $\delta V = 1$, then Equation (6) can be simplified as follows:

$$\rho \Delta u = \rho \delta V g - \nabla p - 2\Omega \times u - \rho a u. \tag{7}$$

The pressure equation for an ideal gas is as follows:

$$P = \rho R T, \tag{8}$$

where $P$ is pressure; $R$ is the ideal gas coefficient; $T$ is the temperature. Substituting Equation (8) into Equation (7) yields:

$$\Delta u = g - \nabla p \frac{RT}{P_{\text{cur}}} - \frac{2\Omega \times uRT}{P_{\text{cur}}} - au. \tag{9}$$

The position and velocity of air particles will change in each iteration to explore new space. Hence, the following equation:

$$\Delta u = u_{\text{new}} - u_{\text{cur}}. \tag{10}$$

And for the vectors $g$ and $\nabla p$ by size and direction can be obtained as follows:

$$g = |g|(0 - x_{\text{cur}}), \tag{11}$$

$$-\nabla p = \left|p_{\text{opt}} - p_{\text{cur}}\right|\left(x_{\text{opt}} - x_{\text{cur}}\right), \tag{12}$$

where $p_{\text{opt}}$ is the optimal pressure value; $p_{\text{cur}}$ is the current pressure value of the particle point; $x_{\text{opt}}$ is the optimal position; $x_{\text{cur}}$ is the current location. The current iteration velocity value of the current iteration velocity is used by the current iteration velocity value $u_{\text{cur}}$, which is derived from the following equation:

$$u_{\text{new}} = (1 - a)u_{\text{cur}} - gx_{\text{cur}} + \left(\frac{RT}{p_{\text{cur}}}\left|p_{\text{opt}} - p_{\text{cur}}\right|\left(x_{\text{opt}} - x_{\text{cur}}\right)\right) + \left(\frac{-2\Omega \times uRT}{p_{\text{cur}}}\right). \tag{13}$$

The air particle velocity is expressed in $u_{\text{cur}}^{\text{otherdim}}$, literature [20] sets the constant to $c = -2|\Omega|R$. Instead of $p_{\text{opt}}$ and $p_{\text{cur}}$, $i$ is used to represent the descending order of all air particles. When $x_{\text{opt}}$ is in position, the pressure value is the minimum and $p_{\text{opt}}$ is 1, then the equation of velocity updating and position updating is as follows:

$$u_{\text{new}} = (1 - a)u_{\text{cur}} - gx_{\text{cur}} + \left(RT\left|1 - \frac{1}{i}\right|\left(x_{\text{opt}} - x_{\text{cur}}\right)\right) + \left(\frac{cu_{\text{cur}}^{\text{otherdim}}}{i}\right), \tag{14}$$

$$x_{\text{new}} = x_{\text{cur}} + (u_{\text{new}} \times \Delta t). \tag{15}$$

The time interval is 1, and for the air quality points in each dimension, the location range of the search can be set according to the specific problem, and the speed of the update has a certain scope, which can be used to make the following judgment of the velocity value size:

$$u_{\text{new}}^{*} = \begin{cases} u_{\max} & u_{\text{new}} > u_{\max} \\ -u_{\max} & u_{\text{new}} < -u_{\max} \end{cases}, \tag{16}$$

where $u_{\max}$ is the speed boundary value.

For the application of the WDO algorithm, the actual position of air particle in the air corresponds to a solution of the problem, and then its fitness is calculated by the pressure value of the position, and finally, it is put into Equations (14) and (15) to iteratively search for the optimal solution. For Equation (14), the first term represents the effect of friction; that is, friction always reduces the original air particle velocity. The second term represents the effect of gravity. The velocity component is directed to the origin of coordinates, which can ensure that air particles will not fall into the boundary position to improve the global search capability. The third term represents the effect of pressure gradient force. When $i = 1$, the pressure value is the minimum. Therefore, the closer the air particle is to the current optimal solution, the smaller its velocity increment will be. The fourth represents the effect of the Coriolis force, which mainly simulates the effect of other dimensional forces on the current dimensional velocity to enhance the robustness of the algorithm.

## 3. The Improved WDO Algorithm

A meta-heuristic algorithm called WDO is based on swarm intelligence. Exploration and exploitation are the two activities of swarm intelligence algorithms. Exploration is to create a person at random in the search space to investigate a potential solution that is not immediately next to the current best solution, which aids in leaving the present local optima. Utilizing local search to conduct a local search in a promising region and speed up algorithm convergence involves looking for potential solutions in a limited area close to the current optimal solution. The challenging problem of how to strike a balance between exploration and exploitation is the main objective of optimizing the algorithm. This paper provides a new improved method. First, chaotic mapping is used to initialize air particles so that they are evenly distributed in space. Second, air particles are mutated according to the model value of hyperbolic tangent. Accordingly, CHTWDO is proposed based on these three improvements.

*3.1. Chaotic Mapping.* Chaotic mapping is mainly used to generate chaotic sequences, which can change simple deterministic systems into random sequences. In the field of algorithmic optimization, chaotic maps are used to replace pseudorandom number generators to produce a batch of chaotic numbers between 0 and 1 [36]. Numerous

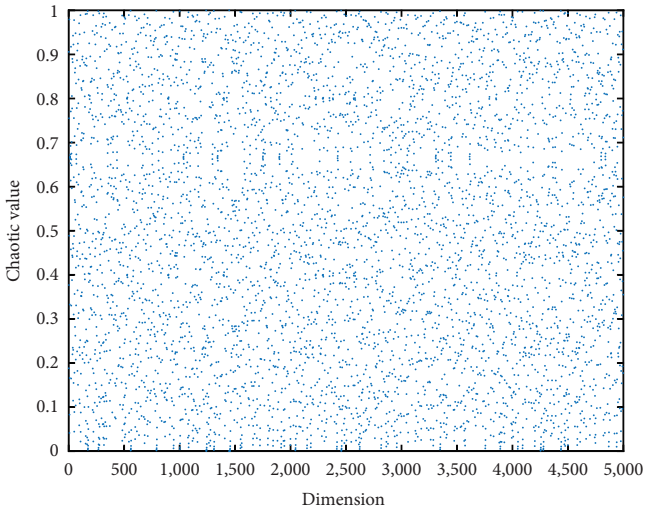


Figure 2: Initial population based on the tent map.

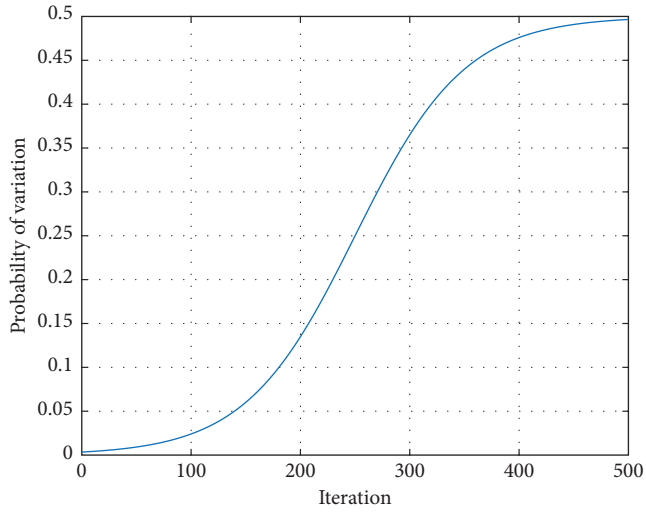


Figure 3: Hyperbolic tangent variation probability.

experiments have verified that the initialization of a population through a chaotic sequence will affect the whole process of the optimization algorithm so that better results can be obtained than pseudorandom numbers [37].

Therefore, this paper uses a chaotic mapping strategy to improve the initialization process of wind particles. The common chaotic mapping mainly includes logistic mapping, cat mapping, and tent mapping. We choose tent mapping here because tent chaotic mapping has advantages over other maps in ergodic, uniform, and iterative speed [38].

The equation for tent mapping to generate chaotic particle sequences is shown in Equation (17).

$$x_{t+1}^{i} = \begin{cases} 2x_t^i & 0 \le x_t^i \le 0.5 \\ 2(1 - x_t^i) & 0.5 < x_t^i \le 1 \end{cases}, \tag{17}$$

where $i = 1, 2\ldots N$ represents the population number; $t = 1, 2\ldots M$ stands for space dimension. Figure 2 shows the initial population based on the tent map.

According to Equation (17), $N$ initial values can be selected, $n$ chaotic sequence $x_t^i$, and then substituted in Equation (18) inverse to the search space, and obtained a uniform random initialization of the air proton.

$$y_t^i = lb_i + (ub_i - lb_i)x_t^i, \tag{18}$$

where $lb_i$ and $ub_i$ are the boundaries of the search range of $x_t^i$.

*3.2. Hyperbolic Tangent Model.* After years of research and development, scholars have put forward some new variation methods, such as exponential, quadratic, and cosine functions, on the basis of the original. After repeated comparison, the CHTWDO algorithm adopts the hyperbolic tangent mobility model, whose equation is as follows:

$$\lambda_k = \frac{P}{2}\left(1 + \frac{\alpha^{k-\frac{n}{2}} - \alpha^{-k+\frac{n}{2}}}{\alpha^{k-\frac{n}{2}} + \alpha^{-k+\frac{n}{2}}}\right), \tag{19}$$

where $\lambda_k$ represents the variation rate; $P$ represents the maximum variation rate; $\alpha$ is the influence factor parameter; $k$ and $n$ represent the current and maximum number of air proton iterations, respectively.

With $P = 0.5$, $n = 500$, and $a = 1.01$, variation probabilities of different iterations can be obtained, and the results are shown in Figure 3. In the initial stage, due to the adoption of chaotic mapping, air particles are evenly distributed in the whole space, so the mutation probability is small in the initial stage, but with the increase of iteration times, the mutation probability increases nonlinearly to ensure the convergence speed and search range. In the final stage, the mutation probability is close to the maximum value to avoid falling into the extreme point.

*3.3. T-Distribution Variation Strategy.* In probability theory and mathematical statistics, the $T$-distribution is often used in terms of the mean of a small sample with unknown variance and a sample that is basically a normal distribution [39]. The $T$-distribution, also known as the student distribution, has a probability density function for $n$ degrees of freedom. The equation is as follows:

$$p_t(x) = \frac{\Gamma\left(\frac{n+1}{2}\right)}{\sqrt{n\pi} \times \Gamma\left(\frac{n}{2}\right)} \times \left(1 + \frac{x^2}{n}\right)^{\frac{n}{2}} \quad -\infty < x < +\infty. \tag{20}$$

If the parameter $n$ of freedom is 1, $t(n = 1) = C(0, 1)$, then the $T$-distribution is the Cauchy distribution. When the degree of freedom parameter $n$ increases along the $X$-axis, the $T$-distribution gradually approaches the normal distribution. When the final degree of freedom parameter $n$ goes to $\infty$, the $T$-distribution is the Gaussian distribution. Therefore,

the Cauchy distribution and the standard Gaussian distribution can be considered as two special cases of $T$-distribution.

The probability of $T$-distribution variation depends on the hyperbolic tangent model. For each air proton, a random number between (0,1) will be generated. If the air proton whose random number is less than the hyperbolic tangent value of the iteration number is the air proton meeting the variation condition, the position update will be completed. The equation is as follows:

$$x_i^t = x_i + x_i \times t(\text{iteration}), \tag{21}$$

where $x_i^t$ is the position of air proton after the $i$ is disturbed only by $T$-distribution; $x_i$ is the position of the ith air proton; $t(\text{iteration})$ is a $T$-distribution whose degree of freedom parameter is the number of iterations.

At the early stage of CHTWDO iteration, the iteration value is small, and the $T$-distribution variation is close to the Cauchy distribution. In this case, variation has a larger effect and strong disturbance ability to air proton position, which can greatly improve the diversity of the population and avoid the algorithm falling into local extreme value. Therefore, it has a strong global search ability. When the iteration reaches the later stage, the iteration value increases and the $T$-distribution variation approaches the Gaussian distribution. In this case, the effect of the variation term decreases. Therefore, the algorithm performs local search and has a better convergence speed and accuracy. However, when the algorithm is iterated to the middle stage, the $T$-distribution variation will have the advantages of Cauchy distribution and Gaussian distribution variation, and it can have both global and local searching capabilities of the algorithm.

*3.4. CHTWDO Process.* The CHTWDO process is as follows:

(a) Parameter initialization. The initial population number, the total number of iterations, search space dimension, $T$-distribution mutation probability, and other parameters.

(b) Population initialization. The chaotic particle sequence of tent is generated by Equation (17) and mapped to the search space according to Equation (18) to obtain the initial position of the seagull.

(c) Calculate the fitness of each proton in the initial air and sort it to find the proton position with the best fitness.

(d) Update the position and velocity of the proton according to Equations (1)–(16), check whether the updated position is out of bounds, and adjust the position of the transgressed proton position to the boundary value of the search space.

(e) Calculate the pressure value of air particles in the current iteration (suitable value) and rearrange the population according to the pressure value.

(f) Calculate the probability of the current iteration value according to Equation (19).

(g) Make $T$-distribution variation with the probability of each proton, update its position by Equation (20), calculate the fitness value of the new position, and compare it with the fitness value of the previous generation to find out and save the location of air particles with the best fitness.

(h) Check whether the algorithm runs to the total number of iterations. If the total number of iterations is satisfied, the algorithm ends, and step (i) is executed); If no, perform steps (d)–(g) to search.

(i) Output optimization results.

The pressure value during the last iteration is recorded as the optimal result. Generally, the termination condition is set to a good enough pressure value (adaptive value) or to a preset maximum iteration algebra. Figure 4 shows the flow of the WDO algorithm.

## 4. Experiments

In order to verify the performance of the improved algorithm in this paper, 16 common benchmark test functions are used for simulation and comparison experiments. The experimental running environment was Intel Core TM i5-10400 CPU, 2.90 GHz main frequency, 16 GB memory, Windows 10 64-bit operating system, and MATLAB R2018b simulation software. All parameters here are uniformly set as population number 30 and total number of iterations 300. Considering the randomness of some algorithms, any algorithm is run independently for 30 times. The average value is used to represent the accuracy of the algorithm, and the standard deviation is used to represent the robustness of the algorithm. The optimal value of the function is shown in bold.

*4.1. Benchmark Functions.* Table 1 shows the eight benchmark functions used for testing. Here, f1–f8 is a single-peak test function, which can measure the accuracy and convergence speed of the algorithm; f9–f14 is a multipeak test function; f15–f24 is a fixed-dimension multipeak test function, which can measure the global search of the algorithm and the ability to avoid falling into the local optimal solution.

*4.2. Comparison with Basic WDO and Several Other Algorithms.* To preliminarily verify the superiority of CHTMDO, seven algorithms, GWO [40], WOA, BA, DA, PSO, IA [41], and basic MDO, are selected for comparison. PSO and BA algorithms are classical optimization algorithms, while DA, GWO, IA, and WOA algorithms are emerging optimization algorithms in recent years, which contain abundant and innovative scientific achievements in the field of meta-heuristic algorithm research and are often used in the comparison process of algorithm performance test [42]. Therefore, these six algorithms are selected as the control group in this paper. Verify the effectiveness of the improvement policy in CHTWDO. Tables 2 and 3, respectively, show the comparison results of mean values and standard deviations on 14 test functions in the low-dimensional search space, where f1–f14 is 30-dimensional, and f15–f24 is fixed-dimensional count. Meanwhile, in order to more intuitively compare the performance of the seven algorithms, the convergence curves of

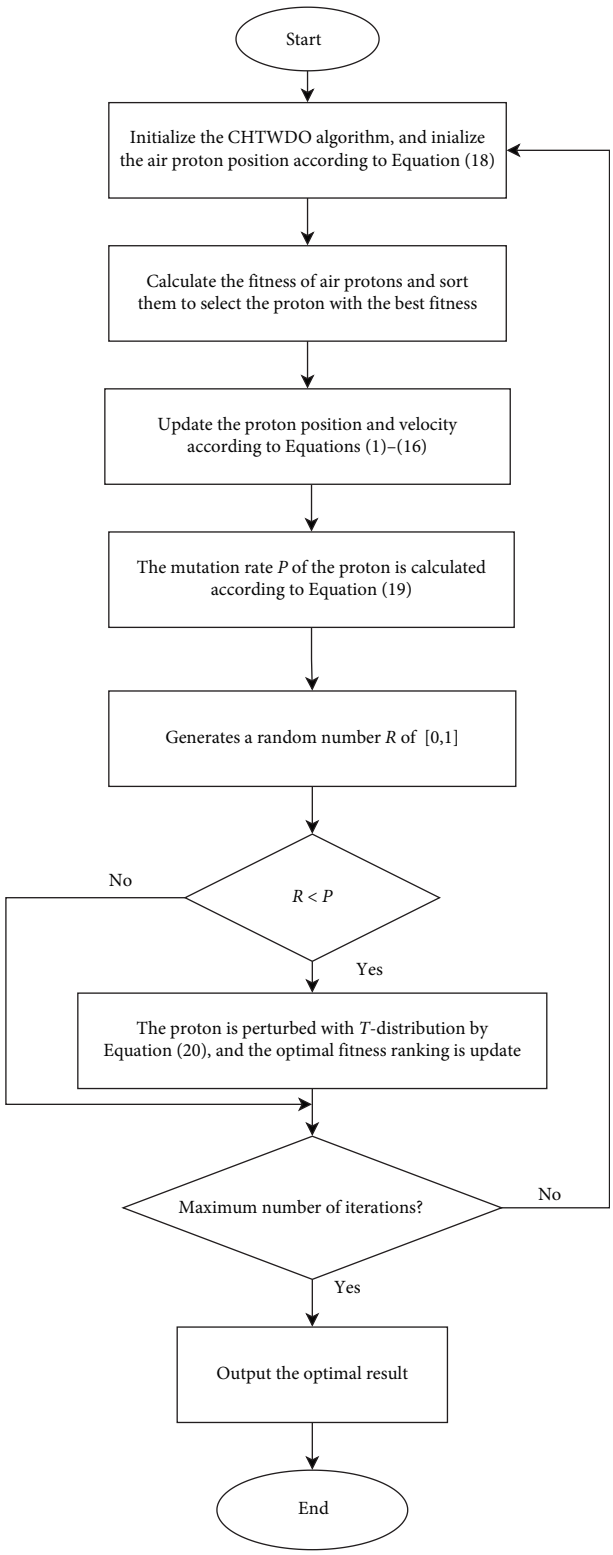


Figure 4: Flowchart of CHTWDO.

the seven optimization algorithms in 24 test functions in low dimension are shown in Figure 5(a)–5(x).

As can be seen from Table 2, the CHTWDO algorithm is in f1, f3, f5, f6, f7, f8, f13, f14 seven test letters. It is obviously superior to the other six algorithms and has higher solving accuracy. Especially for the function f1, compared with WDO, the convergence accuracy is improved by more than 200 orders of magnitude, and for the functions f3, f5, f6, it is also improved by more than 25 orders of magnitude. On functions f2, f9,f10, f18,f20, and f21, CHTWDO and WDO both find the theoretical optimal value. It can be seen from Figure 5(a)–5(x) that the CHTWDO algorithm has a faster convergence speed. In the functions f1–f8 and f10–f24, compared with the other six algorithms, CHTWDO shows extremely fast convergence speed and global optimization ability. The theoretical extremum is found in about 20 iterations on the functions f2 and f4. Only functions f9 and f16 are weaker than GWO and WOA. However, the function f5 and f6 CHTWDO show strong jumping ability in the middle and late stages, indicating that the probability of tangent function and $T$-distribution mutation strategy help the algorithm to jump out of the local optimal solution. However, in functions f9 and f16, CHTWDO and WDO are the same, neither of which jumps out of the local extremum again. As can be seen from Table 3, CHTWDO has good robustness on the basis of improving convergence speed and accuracy. For functions f3–f8 and f10–f12, the robustness of the CHTWDO algorithm is much better than other algorithms, including MWO. On functions f2, f9, f13, f14, and f16–f24, CHTWDO is slightly more robust than other algorithms. For function f15, CHTWDO is slightly less robust than BA, but it is still improved compared with WDO.

Tables 4 and 5, respectively, show the comparison results of the mean and standard deviation of 14 test functions in the high-dimensional search space (100 dimensional). As can be seen from Table 4, CHTWDO has the following performance in optimization accuracy under high-dimensional conditions: First, it is superior to other algorithms in f1, f3–f8, f11, f13, and f14 test functions. Among them, for function f1, the solving accuracy is improved by about 140 orders of magnitude compared with WDO, and for function f3–f5, it is also improved by at least 10 orders of magnitude compared with WDO, which is obviously better than the other five algorithms. Second, in terms of functions f10 and f12, CHTWDO has the same solving accuracy as MWO, but it is still significantly better than the other five algorithms. On the functions f4 and f10–f12, CHTWDO can be solved to the theoretical optimal value. On functions f2 and f9, the performance of CHTWDO and WDO trapped in the same local extreme value is slightly worse than that of GWO and WOA. As can be seen from Table 5, the CHTMWO algorithm has the following performance in robustness under high-dimensional conditions: First, in functions f1, f3–f8, and f10–f14, the CHTMWO algorithm has more advantages than the other seven algorithms, indicating that the algorithm is more stable. Second, in terms of functions f2 and f9, although the robustness of CHTMWO is slightly lower than that of GWO and WOA algorithms, it is still improved compared with MWO.

By combining the optimal values and standard deviations of 30 and 100 dimensions, we sorted the eight algorithms, as shown in Figure 6. By comprehensive comparison, it can be seen that the CHTWDO algorithm has obvious advantages

Table 1: Benchmark functions.

| Function | Equation | Range | Optimal solution |
|---|---|---|---|
| f1 | $f_1(x) = \sum_{i=1}^{n} x_i^2$ | $\pm 100$ | 0 |
| f2 | $f_2(x) = \sum_{i=1}^{n=1} [100(x_{i+1} - x_i^2)^2 + (x_i - 1)^2]$ | $\pm 30$ | 0 |
| f3 | $f_3(x) = \sum_{i=1}^{n} \lvert x_i \rvert + \prod_{i=1}^{n} \lvert x_i \rvert$ | $\pm 10$ | 0 |
| f4 | $f_4(x) = \sum_{i=1}^{n} (\lvert x_i + 0.5 \rvert)^2$ | $\pm 100$ | 0 |
| f5 | $f_5(x) = \sum_{i=1}^{n} \lvert x_i \rvert^{(i+1)}$ | $\pm 1$ | 0 |
| f6 | $f_6(x) = \sum_{i=1}^{n} i x_i^2$ | $\pm 10$ | 0 |
| f7 | $f_7(x) = \sum_{i=1}^{n} \lvert x_i \rvert + \prod_{i=1}^{n} \lvert x_i \rvert$ | $\pm 10$ | 0 |
| f8 | $f_8(x) = \sum_{i=1}^{n} (\sum_{j=1}^{i} x_j)^2$ | $\pm 100$ | 0 |
| f9 | $f_9(x) = \sum_{i=1}^{n} (x_i^2 - 10\cos(2\pi x_i) + 10)$ | $\pm 5.12$ | 0 |
| f10 | $f_{10}(x) = -20\exp(-0.2\sqrt{\frac{1}{n}\sum_{i=1}^{n} x_i^2}) - \exp(\frac{1}{n}\sum_{i=1}^{n} \cos(2\pi x_i)) + 20 + e$ | $\pm 32$ | 0 |
| f11 | $f_{11}(x) = \sum_{i=1}^{n} (10^{\frac{i-1}{n-1}} x_i)^2 - 10\cos(2\pi 10^{\frac{i}{n-1}} x_i) + 10$ | $\pm 5.12$ | 0 |
| f12 | $f_{12}(x) = \frac{1}{4000}(\sum_{i=1}^{n} (x_i - 100)^2) - (\prod_{i=1}^{n} \cos(\frac{x_i - 100}{\sqrt{i}})) + 1$ | $\pm 600$ | 0 |
| f13 | $f_{13}(x) = \sum_{i=1}^{n} (\sum_{k=0}^{k\max} [a^k \cos(2\pi b^k (z_i + 0.5))]) - n\sum_{k=0}^{k\max} [a^k \cos(2\pi b^k \cdot 0.5)]$ $a = 0.5,\ b = 3,\ k\max = 20$ | $\pm 0.5$ | 0 |
| f14 | $f_{14}(x) = \frac{1}{n}\sum_{i=1}^{n} [x_i^4 - 16x_i^2 + 5x_i]$ | $\pm 5$ | $-78.3323$ |
| f15 | $f_{15}(x) = -\sum_{i=1}^{5} [(x - a_i)(x - a_i)^T + c_i]^{-1}$ | $[0,\ 10]^4$ | $-10.1532$ |
| f16 | $f_{16}(x) = \sum_{i=1}^{11} [a_i - \frac{x_1(b_i^2 + b_i x_2)}{b_i^2 + b_i x_3 + x_4}]$ | $[-5,\ 5]^4$ | 0.0003075 |
| f17 | $f_{17}(x) = (\frac{1}{500} + \sum_{j=1}^{25} \frac{1}{j + \sum_{i=1}^{n} (x_i - a_{ij})^6})^{-1}$ | $\pm 65.536$ | 1 |
| f18 | $f_{18}(x) = 4x_1^2 - 2.1x_1^4 + \frac{1}{3}x_1^6 + x_1 x_2 - 4x_2^2 + 4x_2^4$ | $\pm 5$ | $-1.316285$ |
| f19 | $f_{19}(x) = (x_2 - \frac{5.1}{4\pi^2} x_1^2 + \frac{5}{\pi} x_1 - 6)^2 + 10(1 - \frac{1}{8\pi})\cos x_1 + 10$ | $-5 \le x_1 \le 10$ $0 \le x_2 \le 15$ | 0.398 |
| f20 | $f_{20}(x) = -\sum_{i=1}^{4} c_i \exp[-\sum_{j=1}^{3} a_{ij}(x_j - p_{ij})^2]$ | $0 \le x_i \le 1$ | $-3.86$ |
| f21 | $f_{21}(x) = -\sum_{i=1}^{4} c_i \exp[-\sum_{j=1}^{6} a_{ij}(x_j - p_{ij})^2]$ | $0 \le x_i \le 1$ | $-3.32$ |
| f22 | $f_{22}(x) = -\sum_{i=1}^{5} [(x - a_i)(x - a_i)^T + C_i]^{-1}$ | $0 \le x_i \le 10$ | $-10$ |
| f23 | $f_{23}(x) = -\sum_{i=1}^{7} [(x - a_i)(x - a_i)^T + C_i]^{-1}$ | $0 \le x_i \le 10$ | $-10$ |
| f24 | $f_{24}(x) = -\sum_{i=1}^{10} [(x - a_i)(x - a_i)^T + C_i]^{-1}$ | $0 \le x_i \le 10$ | $-10$ |

on more than 80% of test functions in the search space of both low and high dimensions, and the increase of dimension has little influence on the optimization results of CHTWDO.

Table 6 displays the $p$-values for each test function in Wilcoxon's rank sum test comparing CHTWDO with alternative methods according to Table 2. A $p$-value of less than $\alpha = 0.05$ often indicates that there are clear differences between the two sets of data. "+" in this case denotes the superior performance of the compared method above the suggested CHTWDO algorithm. A "=" indicates that the performance of the two algorithms is consistent, while a "−" shows that the comparative method performs worse than the CHTWDO algorithm.

According to the overall ranking rates (Friedman mean test) shown in Figure 7, we observe that the CHTWDO achieves the best rank of 1.083, followed by WDO, WOA, GWO, BA, DA, IA, and PSO, respectively.

*4.3. Comparison to WDO with a Single Improvement Policy.* In order to compare the contribution of three improvement strategies to CHTWDO and verify the effect of a single improvement strategy on WDO optimization, the WDO initialized by tent Chaos is named CWDO, and the WDO algorithm with $T$-distribution variation perturbation is named TWDO. HTWDO with hyperbolic tangent $T$-distribution variation perturbation is compared with the CHTWDO algorithm. The mean value is shown in Table 7, and the standard deviation is shown in Table 8.

As can be seen from Table 7, the optimization accuracy of CHTWDO integrated with three improved strategies in functions f1–f3, f4–f10, and f12–f16 is better than that of WDO improved with a single strategy, and the optimization accuracy of CHTWDO in functions f4 and f11 is the same as that of the other three algorithms. On the function f4, all the four algorithms find the optimal solution. Moreover, it can be found from the comparison that the HTWDO with hyperbolic tangent is superior to TWDO in functions f1–f3, f5–f10, and f12–f16, while the two algorithms are equivalent in f4 and f11. Therefore, it is proved that the optimal solution can be found more effectively according to the probabilistic variation of hyperbolic tangent than the fixed probabilistic variation. As can be seen from Table 7, the robustness of CHTWDO on functions f1–f3, f5–f9, and

Table 2: Comparison of an average of eight algorithms in low dimension.

| Algorithm | f1 | f2 | f3 | f4 | f5 | f6 | f7 | f8 |
|---|---|---|---|---|---|---|---|---|
| CHTWMO | **1.00E − 300** | **1.00E + 02** | **1.52E − 60** | **0** | **2.15E − 10** | **1.47E − 10** | **2.23E − 90** | **2.24E − 58** |
| WMO | 4.21E − 82 | 1.01E + 02 | 8.70E − 16 | 1.26E + 02 | 2.81E − 02 | 1.55E − 02 | 1.98E − 60 | 5.88E − 28 |
| GWO | 4.72E − 42 | 1.03E + 02 | 1.12E − 01 | 2.18E + 01 | 5.24E − 03 | 2.93E − 03 | 1.84E − 30 | 9.94E − 02 |
| WOA | 2.59E − 65 | **1.00E + 02** | 6.09E − 01 | 1.36E + 01 | 1.79E − 02 | 9.56E − 03 | 2.25E − 15 | 1.46E + 00 |
| BA | 5.54E − 33 | 2.26E + 03 | 2.11E − 09 | 1.17E + 01 | 2.84E − 02 | 6.34E − 03 | 3.64E − 02 | 9.97E − 01 |
| DA | 1.12E − 23 | 1.00E + 05 | 9.41E − 07 | 3.85E + 02 | 1.22E − 02 | 3.87E − 05 | 7.66E − 07 | 1.06E + 01 |
| PSO | 1.97E − 19 | 1.02E + 04 | 7.97E − 11 | 4.36E + 02 | 7.97E − 01 | 2.49E − 02 | 4.59E − 04 | 6.25E + 00 |
| IA | 5.88E − 08 | 4.28E + 02 | 8.34E − 02 | 8.19E + 02 | 6.43E − 01 | 4.78E − 03 | 1.35E − 07 | 4.40E + 00 |
| | f9 | f10 | f11 | f12 | f13 | f14 | f15 | f16 |
| CHTWMO | 1.21E − 10 | **1.08E − 15** | **1.15E − 15** | **1.35E − 15** | **8.08E − 13** | **−1.01E + 02** | **−1.02E + 01** | 3.30E − 04 |
| WMO | 1.30E − 10 | 1.87E − 15 | 1.88E − 15 | 1.96E − 15 | 5.61E − 07 | −2.99E + 01 | −1.00E + 01 | 3.88E − 04 |
| GWO | **1.04E − 10** | 1.79E − 10 | 2.32E − 08 | 2.18E − 07 | 2.24E − 04 | −2.93E + 01 | −8.32E + 00 | 5.11E − 04 |
| WOA | 1.53E − 02 | 2.04E − 05 | 2.59E − 05 | 2.52E − 05 | 7.79E − 04 | −2.76E + 01 | −9.91E + 00 | **3.26E − 04** |
| BA | 6.24E − 03 | 1.09E − 01 | 2.51E − 04 | 1.54E − 05 | 2.21E − 04 | −2.63E + 01 | −9.92E + 00 | 5.69E − 04 |
| DA | 2.07E − 01 | 7.64E − 01 | 4.41E − 03 | 1.51E − 04 | 2.22E − 02 | −3.83E + 01 | −8.83E + 00 | 3.56E − 04 |
| PSO | 2.67E-03 | 2.84E − 01 | 1.40E − 02 | 1.24E − 02 | 2.27E − 01 | −3.38E + 01 | −7.65E + 00 | 2.05E − 03 |
| IA | 1.98E − 02 | 1.28E − 01 | 1.31E − 01 | 1.80E − 01 | 6.43E − 01 | −6.88E + 01 | −9.28E + 00 | 6.10E − 03 |
| | f17 | f18 | f19 | f20 | f21 | f22 | f23 | f24 |
| CHTWMO | 7.96E − 01 | **−1.03E + 00** | **3.98E − 01** | **−3.86E + 00** | **−3.26E + 00** | **−1.02E + 01** | **−9.87 E + 00** | **−9.87 E + 00** |
| WMO | 9.73E − 01 | **−1.03E + 00** | 4.03E − 01 | **−3.86E + 00** | **−3.26E + 00** | −9.99E + 00 | −9.82 E + 00 | −9.86 E + 00 |
| GWO | 8.43E − 01 | **−1.03E + 00** | 4.11E − 01 | −3.85E + 00 | −3.25E + 00 | −8.05E + 00 | −9.74 E + 00 | −8.89 E + 00 |
| WOA | 4.74E − 01 | −1.01E + 00 | 1.71E + 01 | −3.85E + 00 | −3.24E + 00 | −9.58E + 00 | −9.81 E + 00 | −9.81 E + 00 |
| BA | 6.52E − 01 | −0.99E + 00 | 5.03E − 01 | −3.84E + 00 | −3.23E + 00 | −9.65E + 00 | −4.95 E + 00 | −9.42 E + 00 |
| DA | 6.80E − 01 | −1.01E + 00 | 3.99E − 01 | −3.83E + 00 | −3.17E + 00 | −8.93 E + 00 | −6.89 E + 00 | −9.02 E + 00 |
| PSO | 3.93E − 01 | −1.02E + 00 | 3.99E − 01 | −3.73E + 00 | −2.88E + 00 | −7.46E + 00 | −8.98 E + 00 | −6.69 E + 00 |
| IA | **8.16E − 02** | −1.01E + 00 | 7.22E − 01 | −3.81E + 00 | −2.67E + 00 | −9.42E + 00 | −3.79 E + 00 | −4.96 E + 00 |

The significance of bold values represent the optimal values of each test function.

f13–f16 is better than that of CWDO, TWDO, and HTWDO, and the robustness of CHTWDO on functions f4, f10–f12 is the same as that of CWDO, TWDO, and HTWDO.

As you can see from Figure 8, CHTWDO ranks first in all 16 functions, including a tie for first. The comprehensive comparison shows that CHTWDO has absolute superiority in 81% of the test functions and has the same optimization performance as CWDO, TWDO, and HTWDO in 19% of the test functions. However, HTWDO outperforms TWDO on 88% of the functions and has the same optimization performance on 12% of the functions. However, the three single algorithms are better than ordinary WDO. The results show that the CHTWDO integrated with the three improved strategies has more advantages than the CWDO, TWDO, and HTWDO of other strategies, which can improve the optimization accuracy and convergence speed while ensuring the stability of the algorithm. By comparing the contribution degree of a single strategy on CHTWDO, it is found that the chaotic initialization strategy can make the algorithm jump out of the local extreme value stably and repeatedly and improve the convergence accuracy. The $T$-distribution mutation strategy can improve the optimization accuracy and convergence speed, obviously, but the stability is poor. Hyperbolic tangent variation can ensure that the convergence speed is improved in the early stage and the ability to jump out of the extreme point is enhanced in the late stage. Combining the advantages of the three improvement strategies, the optimization accuracy and convergence speed of CHTWDO can be significantly improved, and the stability is high.

*4.4. Comparison of WDO Improvement with Other Scholars.* In order to further test the performance of CHTWDO, the improved WDO in this paper is compared with that of other scholars, and the comparison results are shown in Table 9.

As can be seen from Table 9, compared with WDO improved by other scholars, CHTWDO shows absolute superiority in functions f1, f4, and f10, and its optimization accuracy and robustness are far superior to those of the other three literatures. The solution results of functions f2, f3, f6, f8, f9, f12–f15 are better than those of the other three papers. However, the optimization accuracy and robustness of functions f5, f7, f11, and f16 are inferior to the improved WDO algorithm proposed in other literatures.

*4.5. The Center-Bias Problem.* We use the same method used in literature [43] to reveal the central deviation problem. The eight benchmark functions (f1–f8) used in our tests are shown in Table 1. It can be easily seen that many of these functions have corresponding optimal values at or very close to the zero vector. For evaluation, we set the dimension of the problem to 30 and allow up to 50,000 function evaluations. We also chose a simple performance metric—the average

Table 3: Comparison of the standard deviation of eight algorithms in low dimension.

| Algorithm | f1 | f2 | f3 | f4 | f5 | f6 | f7 | f8 |
|---|---|---|---|---|---|---|---|---|
| CHTWDO | **1.31E − 300** | **1.01E + 02** | **2.23E − 60** | **0** | **3.11E − 10** | **1.32E − 10** | **2.81E − 90** | **2.89E − 58** |
| WDO | 5.79E − 82 | 1.14E + 02 | 1.26E − 15 | 1.01E + 02 | 3.14E − 02 | 1.74E − 02 | 2.35E − 60 | 3.90E − 28 |
| GWO | 2.99E − 42 | 1.36E + 02 | 9.85E − 02 | 2.35E + 01 | 2.81E − 03 | 2.04E − 03 | 1.52E − 30 | 9.74E − 02 |
| WOA | 4.36E − 64 | 3.55E + 02 | 7.84E − 01 | 1.34E + 01 | 2.51E − 02 | 1.15E − 02 | 3.25E − 15 | 1.33E + 00 |
| BA | 5.68E − 33 | 1.13E + 04 | 1.33E − 08 | 1.20E + 01 | 4.06E − 02 | 3.45E − 03 | 1.95E − 02 | 1.11E + 00 |
| DA | 9.15E − 24 | 1.16E + 04 | 8.81E − 07 | 4.15E + 02 | 5.69E − 04 | 2.65E − 05 | 7.19E − 07 | 1.29E + 01 |
| PSO | 1.45E − 19 | 1.08E + 04 | 1.12E − 10 | 4.14E + 02 | 3.08E − 02 | 1.23E − 02 | 4.04E − 04 | 8.42E + 00 |
| IA | 5.64E − 08 | 7.53E + 02 | 1.03E − 01 | 8.67E ± 02 | 2.73E − 02 | 2.94E − 03 | 1.71E − 07 | 3.52E + 00 |
| | f9 | f10 | f11 | f12 | f13 | f14 | f15 | f16 |
| CHTWDO | **1.00E − 10** | **0** | **0** | **0** | **6.14E − 16** | **8.02E + 01** | 1.05E + 01 | **2.04E − 04** |
| WDO | 1.01E − 10 | 1.45E − 15 | 1.74E − 15 | 1.94E − 15 | 6.03E − 07 | 3.84E + 01 | 1.28E + 01 | 2.96E − 04 |
| GWO | 1.23E − 10 | 9.58E − 11 | 3.31E − 07 | 1.79E − 07 | 1.05E − 04 | 2.43E + 01 | 1.15E + 01 | 3.73E − 04 |
| WOA | 1.82E − 03 | 2.07E − 05 | 3.09E − 05 | 2.78E − 05 | 6.47E − 04 | 2.86E + 01 | 6.08E + 01 | 6.50E − 04 |
| BA | 7.21E − 03 | 7.60E − 02 | 3.24E − 05 | 1.87E − 04 | 2.82E − 04 | 2.16E + 01 | **1.03E + 01** | 3.23E − 04 |
| DA | 1.34E − 01 | 9.14E − 01 | 2.60E − 03 | 5.80E − 03 | 3.13E − 02 | 1.87E + 01 | 8.57E + 01 | 5.94E − 04 |
| PSO | 1.70E − 03 | 1.84E − 01 | 6.98E − 03 | 9.61E − 03 | 2.31E − 01 | 1.43E + 01 | 3.84E + 01 | 4.95E − 03 |
| IA | 1.95E − 02 | 1.07E − 01 | 1.03E − 01 | 9.45E − 03 | 1.05E + 00 | 4.74E + 01 | 7.87E + 00 | 1.25E − 03 |
| | f17 | f18 | f19 | f20 | f21 | f22 | f23 | f24 |
| CHTWDO | **2.08E − 01** | **0** | **1.08E − 01** | **2.90E + 00** | **1.09E + 00** | **1.01E + 00** | **2.05E − 02** | **7.13E − 01** |
| WDO | 5.35E − 01 | 1.18E + 00 | 2.07E − 01 | 3.94E + 00 | 1.20E + 00 | 3.12E + 00 | 1.46E − 01 | 1.56E + 00 |
| GWO | 7.19E − 01 | 1.67E + 00 | 1.96E − 01 | 3.71E + 00 | 2.14E + 00 | 4.08E + 00 | 5.74E − 01 | 3.04E + 00 |
| WOA | 4.46E − 01 | 1.96E + 00 | 8.62E + 00 | 3.08E + 00 | 3.07E + 00 | 3.62E + 00 | 1.83E + 00 | 4.24E + 00 |
| BA | 4.91E − 01 | 2.83E + 00 | 3.12E − 01 | 3.75E + 00 | 4.95E + 00 | 7.32E + 00 | 3.09E + 00 | 2.25E + 00 |
| DA | 3.69E − 01 | 1.51E + 00 | 2.83E − 01 | 4.97E + 00 | 3.86E + 00 | 3.12E + 00 | 4.18E + 00 | 5.16E + 00 |
| PSO | 3.35E − 01 | 3.57E + 00 | 2.37E − 01 | 3.15E + 00 | 2.18E + 00 | 4.47E + 00 | 8.35E − 01 | 8.83E − 01 |
| IA | 6.07E − 00 | 1.64E + 00 | 4.09E − 01 | 5.70E + 00 | 2.83E + 00 | 5.12E + 00 | 3.82E − 01 | 3.06E + 00 |

The significance of bold values represent the optimal values of each test function.

error (the difference between the best function value and the best function value) of 20 independent runs. We refer to the result of the calculation as the "unshifted" result. We then introduce a shift operation, which "moves" the reference function by a predetermined vector $s$, meaning that the function $f(x)$ becomes $f(x+s)$. It is expected that a "small" value of $s$ should not lead to a large deviation in the behavior of the optimization method, because the two problems are very similar. We choose the shift vector as 10% of the range—for example, for F01, $s = [20, 20, \ldots]$. We use the same computational framework (i.e., dimension 30, up to 50,000 function evaluations, and 20 independent runs) and refer to the results of these computations as "shifted" results. So, we get the ratio between shifted and unshifted. For methods that do not include center bias, one would expect the number to be close to 1 (because the shift and shift problems are similar), while for methods that do include center bias, the ratio should be much greater than 1. If the geometric mean of the reference function is greater than 1E + 01, a central deviation operator is considered to exist. The ratio of CHTWDO to WDO is shown in Table 10.

From Table 10, we can find that the geometric mean of CHTWDO is less than 1E + 01, and the shift and nonshift ratios are close to 1. On the other hand, WDO is greater than 1E + 01, especially on f2, the ratio is as high as 4.457E + 02, and other functions f4, f13, f18, f19, and f24 is less than 1E + 01, all of which are greater than 1E + 01. Therefore, CHTWDO improves the defect of WDO in the problem of center bias.

## 5. Engineering Examples

CHTWDO has demonstrated strong competitiveness on conventional test functions through the aforementioned comparisons and analysis. This section will look at possible engineering applications for CHTWDO. We choose CHTWDO and seven additional well-liked algorithms to address four well-known engineering optimization issues. The conclusion will be reached by comparing the output of several algorithms on engineering cases. While HTWDO ranks the first place in f4 and f11, f15, and f16 rank the third, slightly worse than CWDO, and other functions are better than CWDO in the second place. CWDO ranks the first place in f4 and f11, while f15f and f16 are better than HTWDO and TWDO, ranking the second, and the rest are the worst. TWDO is inferior to HTWDO in all functions but superior to CWDO except f4, f11, f15, and f16.

*5.1. Welded Beam Design.* One of the most well-known engineering issues used to evaluate the algorithm's effectiveness is the welded beam design problem, which is a type of composite beam. Figure 9 illustrates how a weld is created by

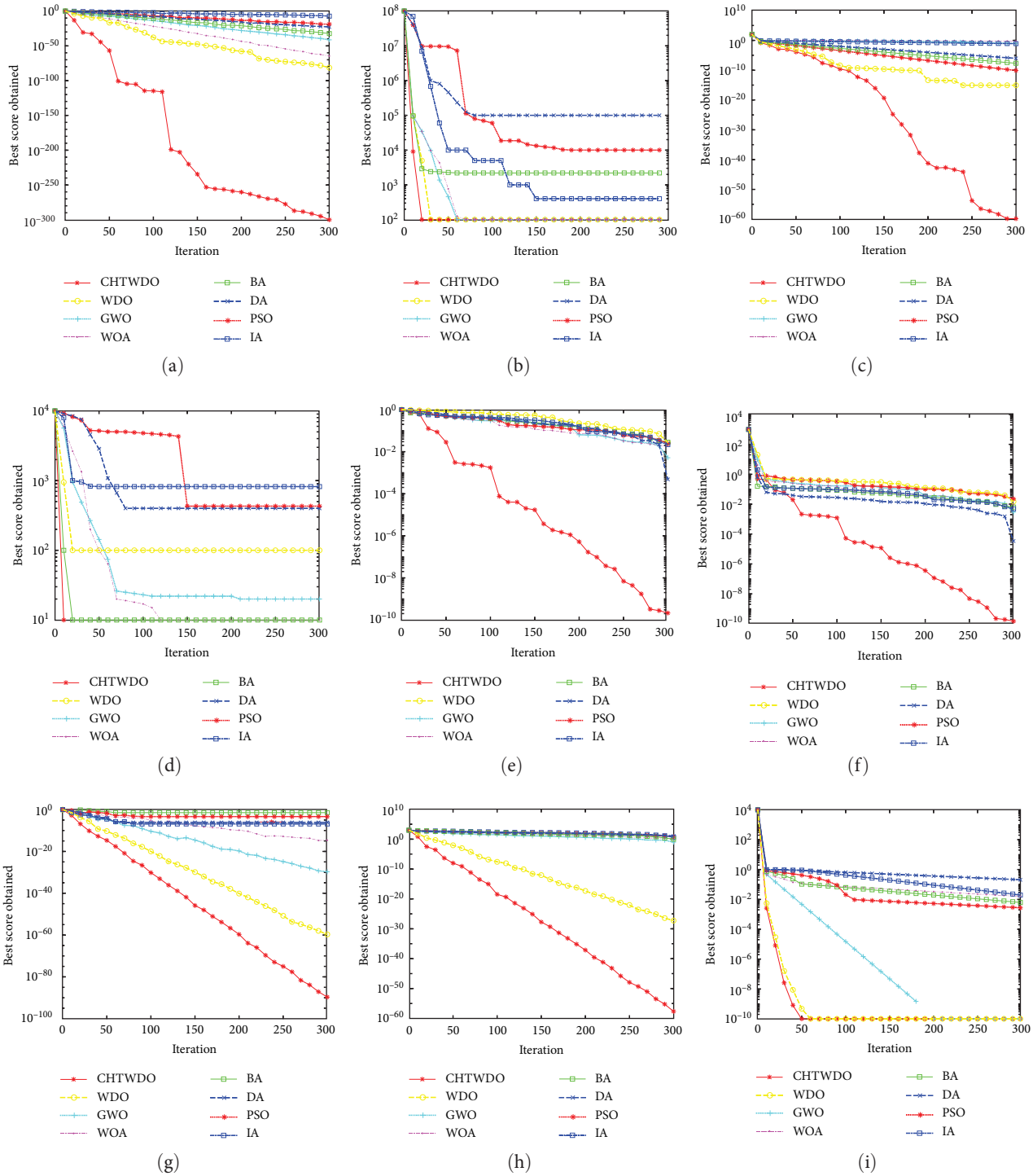


Figure 5: Continued.

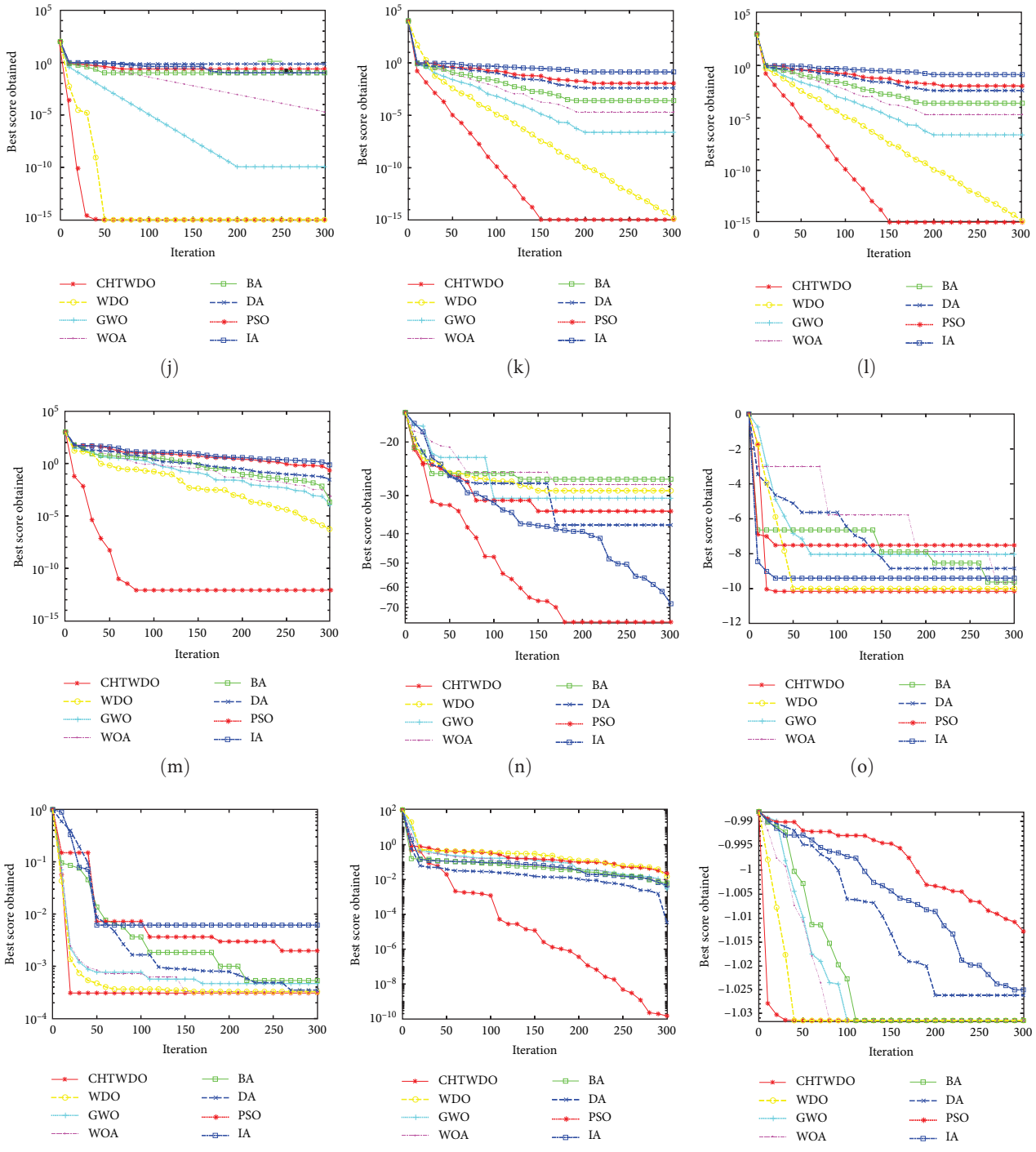


Figure 5: Continued.

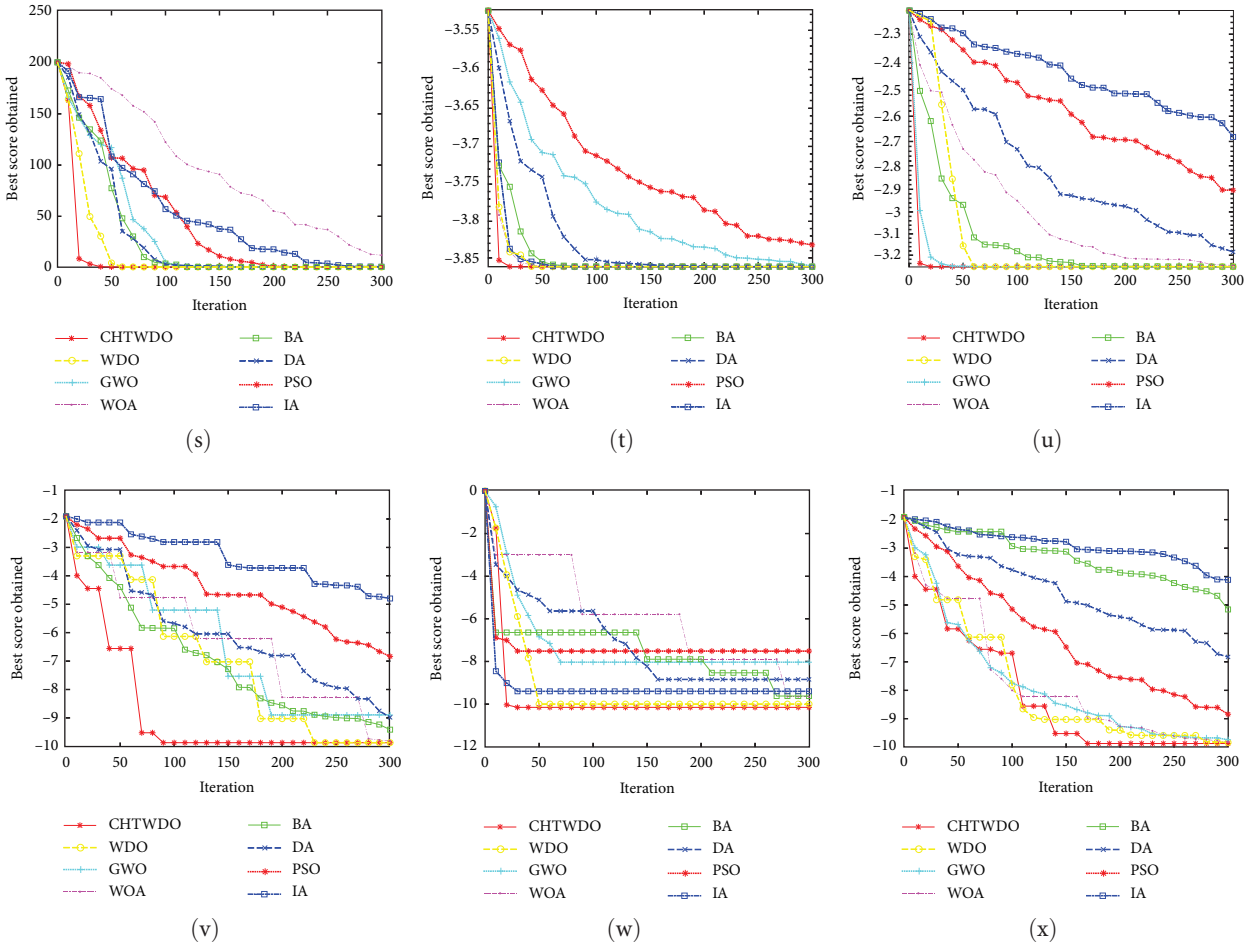


Figure 5: Convergence curves of eight algorithms on 24 test functions in low dimensions: (a) f1; (b) f2; (c) f3; (d) f4; (e) f5; (f) f6; (g) f7; (h) f8; (i) f9; (j) f10; (k) f11; (l) f12; (m) f13; (n) f14; (o) f15; (p) f16; (q) f17; (r) f18; (s) f19; (t) f20; (u) f21; (v) f22; (w) f23; (x) f24.

Table 4: Comparison of the average of eight algorithms in 100 dimensions.

| Algorithm | f1 | f2 | f3 | f4 | f5 | f6 | f7 |
|---|---|---|---|---|---|---|---|
| CHTWDO | **1.74E − 256** | 1.03E + 02 | **1.34E − 60** | **0** | **2.15E − 10** | **1.14E − 08** | **3.41E − 82** |
| WDO | 6.37E − 69 | 4.16E + 02 | 4.24E − 15 | 1.34E + 03 | 2.81E − 02 | 3.64E − 03 | 3.16E − 54 |
| GWO | 8.32E − 40 | 2.13E + 03 | 7.43E − 01 | 5.72E + 01 | 5.20E − 03 | 7.04E − 03 | 3.84E − 28 |
| WOA | 1.53E − 61 | **1.02E + 02** | 8.56E − 01 | 4.07E + 01 | 1.79E − 02 | 1.52E − 03 | 8.62E − 14 |
| BA | 2.15E − 34 | 5.73E + 03 | 4.32E − 09 | 6.58E + 01 | 2.84E − 02 | 1.72E − 02 | 1.84E − 01 |
| DA | 9.04E − 22 | 2.89E + 05 | 4.31E − 06 | 9.40E + 02 | 1.02E − 02 | 8.08E − 04 | 9.01E − 06 |
| PSO | 5.46E − 18 | 1.42E + 05 | 5.52E − 10 | 8.53E + 02 | 7.97E − 01 | 8.32E − 02 | 2.60E − 03 |
| IA | 7.38E − 08 | 6.48E + 02 | 7.80E − 02 | 1.96E + 03 | 6.43E − 01 | 1.29E − 02 | 1.24E − 07 |
| | f8 | f9 | f10 | f11 | f12 | f13 | f14 |
| CHTWDO | **1.06E − 54** | 1.08E − 10 | **0** | **0** | **0** | **8.02E − 15** | **7.16E + 01** |
| WDO | 2.06E − 26 | 1.58E − 10 | **0** | 1.04E − 14 | **0** | 3.94E − 06 | 4.06E + 01 |
| GWO | 5.92E − 02 | **1.04E − 10** | 1.26E − 10 | 2.31E − 06 | 1.79E − 07 | 1.95E − 04 | 3.12E + 01 |
| WOA | 2.67E + 00 | 5.16E − 02 | 8.26E − 05 | 3.13E − 04 | 2.78E − 05 | 4.07E − 04 | 3.15E + 01 |
| BA | 3.94E + 00 | 1.06E − 02 | 9.04E − 02 | 8.08E − 05 | 1.87E − 04 | 5.37E − 04 | 2.74E + 01 |
| DA | 2.06E + 00 | 6.12E − 01 | 9.90E − 01 | 9.26E − 03 | 5.80E − 03 | 9.41E − 01 | 1.98E + 01 |
| PSO | 9.19E + 00 | 8.42E − 03 | 8.97E − 01 | 9.04E −03 | 9.61E − 03 | 7.62E − 01 | 1.85E + 01 |
| IA | 1.04E − 01 | 8.16E − 02 | 3.73E − 01 | 2.92E − 01 | 9.45E − 03 | 2.15E + 00 | 5.38E + 01 |

The significance of bold values represent the optimal values of each test function.

Table 5: Comparison of standard deviations of eight algorithms in 100 dimensions.

| Algorithm | f1 | f2 | f3 | f4 | f5 | f6 | f7 |
|---|---|---|---|---|---|---|---|
| CHTWDO | **1.28E − 240** | 1.68E + 02 | **6.06E − 60** | **0** | **2.08E − 10** | **1.28E − 08** | **5.24E − 80** |
| WDO | 1.08E − 64 | 7.24E + 02 | 8.26E − 15 | 3.24E + 04 | 6.24E − 02 | 6.09E − 03 | 6.78E − 50 |
| GWO | 3.96E − 30 | 8.04E + 03 | 9.12E − 01 | 2.72E + 01 | 4.80E − 03 | 8.14E − 03 | 7.14E − 28 |
| WOA | 1.62E − 62 | **1.25E + 02** | 9.76E − 01 | 6.07E + 01 | 3.84E − 02 | 7.31E − 03 | 3.78E − 12 |
| BA | 4.25E − 34 | 9.69E + 03 | 6.08E − 08 | 7.58E + 01 | 7.14E − 02 | 2.49E − 02 | 9.08E − 01 |
| DA | 9.42E − 22 | 1.75E + 04 | 9.31E − 08 | 9.57E + 01 | 1.84E − 02 | 9.42E − 04 | 1.78E − 05 |
| PSO | 1.18E − 18 | 1.90E + 05 | 8.52E − 11 | 2.36E + 02 | 9.03E − 01 | 9.76E − 02 | 3.62E − 03 |
| IA | 6.73E − 08 | 9.08E + 02 | 1.04E − 03 | 8.90E + 03 | 8.24E − 01 | 1.83E − 02 | 7.92E − 07 |
| | f8 | f9 | f10 | f11 | f12 | f13 | f14 |
| CHTWDO | **8.72E − 50** | 1.47E − 10 | **2.17E− 08** | **9.63E − 18** | **0** | **4.34E − 14** | **6.03E + 01** |
| WDO | 4.04E − 24 | 2.37E − 10 | 1.72E − 14 | 5.17E − 16 | 4.97E − 14 | 3.71E − 06 | 5.16E + 01 |
| GWO | 5.93E − 02 | **1.16E − 10** | 1.86E − 10 | 6.41E − 05 | 1.88E − 07 | 7.15E − 04 | 3.78E + 01 |
| WOA | 8.35E + 00 | 7.23E − 02 | 8.35E − 04 | 2.37E − 03 | 4.14E − 05 | 8.08E − 04 | 3.82E + 01 |
| BA | 7.14E + 00 | 8.16E − 02 | 2.79E − 01 | 9.18E − 04 | 3.77E − 04 | 5.17E − 04 | 1.68E + 01 |
| DA | 4.42E + 00 | 9.37E − 01 | 3.81E + 00 | 2.66E − 02 | 9.70E − 03 | 9.98E − 01 | 4.13E + 01 |
| PSO | 9.82E + 00 | 9.38E − 03 | 7.24E − 01 | 1.34E − 02 | 1.03E − 02 | 8.81E − 01 | 2.17E + 01 |
| IA | 2.37E + 00 | 9.42E − 02 | 5.13E − 01 | 6.93E − 01 | 1.25E − 02 | 7.03E + 00 | 8.04E + 01 |

The significance of bold values represent the optimal values of each test function.

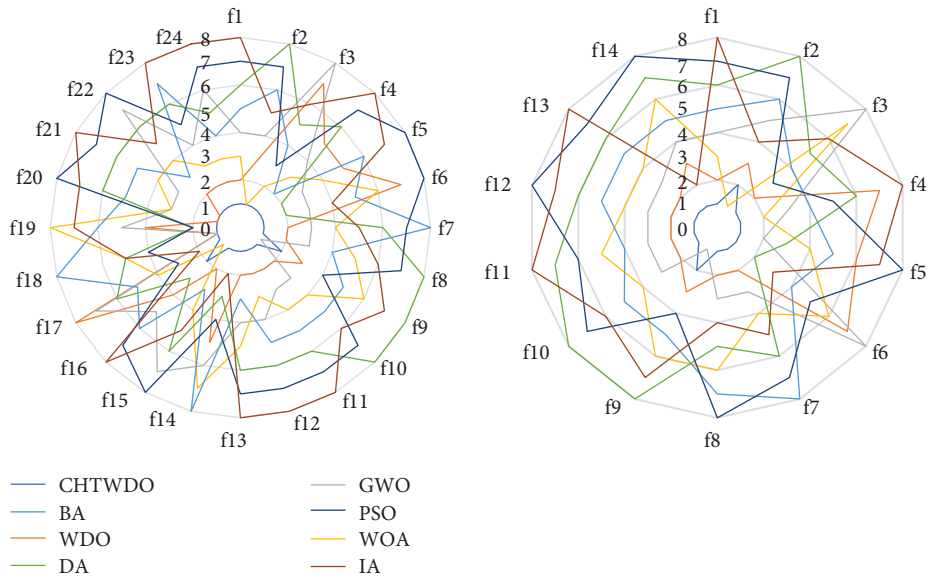


Figure 6: Radar maps of different algorithms.

joining several pieces together using molten metal in the manner shown.

By choosing the best four design variables—bar thickness ($b$), bar length ($l$), weld thickness ($t$), and bar height ($h$)—the best aim is to reduce the overall cost of the beam. The optimization model can be expressed as follows:

Already know: $x = [x_1, x_2, x_3, x_4] = [h, m, t, b]$,

Minimize: $f(x) = 1.10471x_1^2x_2 + 0.04811x_3x_4(14.0 + x_2)$,

Variables range: $0.1 \le x_1 \le 2, 0.1 \le x_2 \le 10, 0.1 \le x_3 \le 10, 0.1 \le x_4 \le 2$,

Restriction condition:

$$\begin{cases} h_1(\boldsymbol{x}) = \tau(x) - \tau_{\max} \le 0, h_2(\boldsymbol{x}) = \sigma(x) - \sigma_{\max} \le 0, \\ h_3(\boldsymbol{x}) = \delta(x) - \delta_{\max} \le 0, h_4(\boldsymbol{x}) = x_1 - x_4 \le 0, \\ h_5(\boldsymbol{x}) = P - P_C(x) \le 0, h_6(\boldsymbol{x}) = 0.125 - x_1 \le 0, \\ h_7(\boldsymbol{x}) = 1.1047x_1^2x_2 + 0.04811x_3x_4(14.0 + x_2) - 5.0 \le 0, \end{cases} \tag{22}$$

where

Table 6: Results of Wilcoxon's rank sum test on 24 benchmark functions.

| | WDO | GWO | WOA | BA | DA | PSO | IA |
|---|---|---|---|---|---|---|---|
| 1 | 6.80E − 08/− | 6.80E − 08/− | 6.80E − 08/− | 6.80E − 08/− | 6.80E − 08/− | 6.80E − 08/− | 6.80E − 08/− |
| 2 | 4.12E − 01/ = | 3.57E − 01/ = | NaN/ = | 6.80E − 08/− | 6.80E − 08/− | 6.80E − 08/− | 2.39E − 08/− |
| 3 | 7.82E − 08/− | 7.82E − 08/− | 7.82E − 08/− | 7.82E − 08/− | 7.82E − 08/− | 7.82E − 08/− | 7.82E − 08/− |
| 4 | 9.24E − 08/− | 9.24E − 08/− | 9.24E − 08/− | 9.24E − 08/− | 9.24E − 08/− | 9.24E − 08/− | 9.24E − 08/− |
| 5 | 8.43E − 09/− | 8.43E − 09/− | 8.43E − 09/− | 8.43E − 09/− | 8.43E − 09/− | 8.43E − 09/− | 8.43E − 09/− |
| 6 | 6.80E − 08/− | 6.80E − 08/− | 6.80E − 08/− | 6.80E − 08/− | 6.80E − 08/− | 6.80E − 08/− | 6.80E − 08/− |
| 7 | 8.94E − 08/− | 6.79E − 08/− | 3.94E − 08/− | 3.31E − 08/− | 9.23E − 08/− | 6.41E − 08/− | 6.70E − 08/− |
| 8 | 6.80E − 08/− | 6.80E − 08/− | 6.80E − 08/− | 6.80E − 08/− | 6.80E − 08/− | 6.80E − 08/− | 6.80E − 08/− |
| 9 | 1.02E − 02/+ | NaN/ = | 3.89E − 06/− | 4.02E − 06− | 3.71E − 06/− | 3.88E − 06/− | 9.73E − 06/− |
| 10 | 8.51E − 01/ = | 8.52E − 01/ = | 6.80E − 08/− | 6.80E − 08/− | 6.80E − 08/− | 6.80E − 08/− | 6.80E − 08/− |
| 11 | 4.72E − 06/− | 6.80E − 08/− | 6.80E − 08/− | 6.80E − 08/− | 6.80E − 08/− | 6.80E − 08/− | 6.80E − 08/− |
| 12 | 5.36E − 07/− | 6.80E − 08/− | 6.80E − 08/− | 6.80E − 08/− | 6.80E − 08/− | 6.80E − 08/− | 6.80E − 08/− |
| 13 | 6.80E − 08/− | 6.80E − 08/− | 6.80E − 08/− | 6.80E − 08/− | 6.80E − 08/− | 6.80E − 08/− | 6.80E − 08/− |
| 14 | 1.14E − 08/− | 1.14E − 08/− | 1.14E − 08/− | 1.14E − 08/− | 1.14E − 08/− | 1.14E − 08/− | 1.14E − 08/− |
| 15 | 6.80E − 08/− | 6.80E − 08/− | 6.80E − 08/− | 6.80E − 08/− | 6.80E − 08/− | 6.80E − 08/− | 6.80E − 08/− |
| 16 | 1.15E − 02/ = | 3.09E − 02/− | NaN/+ | 3.84E − 02/ = | 2.07E − 02/ = | 6.80E − 08/− | 6.80E − 08/− |
| 17 | 5.72E − 02/− | 6.80E − 02/− | 1.49E − 01/+ | 6.35E − 01/+ | 1.28E − 01/+ | 3.69E − 01/+ | NaN/+ |
| 18 | NaN/ = | NaN/ = | 1.00E + 00/ = | 8.76E − 01/− | 1.00E + 00/ = | 1.00E + 00/ = | 1.00E + 00/ = |
| 19 | 6.80E − 08/− | 6.80E − 08/− | 6.80E − 08/− | 6.80E − 08/− | 6.80E − 08/− | 6.80E − 08/− | 6.80E − 08/− |
| 20 | NaN / = | 2.07E − 02/− | 2.07E − 02/− | 2.07E − 02/− | 2.07E − 02/− | 2.07E − 02/− | 2.07E − 02/− |
| 21 | NaN / = | 6.80E − 08/− | 6.80E − 08/− | 6.80E − 08/− | 6.80E − 08/− | 6.80E − 08/− | 6.80E − 08/− |
| 22 | 8.02E − 09/− | 8.02E − 09/− | 8.02E − 09/− | 8.02E − 09/− | 8.02E − 09/− | 8.02E − 09/− | 8.02E − 09/− |
| 23 | 1.25E − 01/ = | 1.31E − 01/− | 1.26E − 01/ = | 9.24E − 04/− | 5.05E − 05/− | 1.69E − 08/ = | 6.80E − 08/− |
| 24 | 6.80E − 08/− | 6.80E − 08/− | 6.80E − 08/− | 6.80E − 08/− | 6.80E − 08/− | 6.80E − 08/− | 6.80E − 08/− |
| +/ = /− | 1/7/16 | 0/4/20 | 2/3/19 | 1/1/22 | 1/2/21 | 1/2/21 | 1/1/22 |

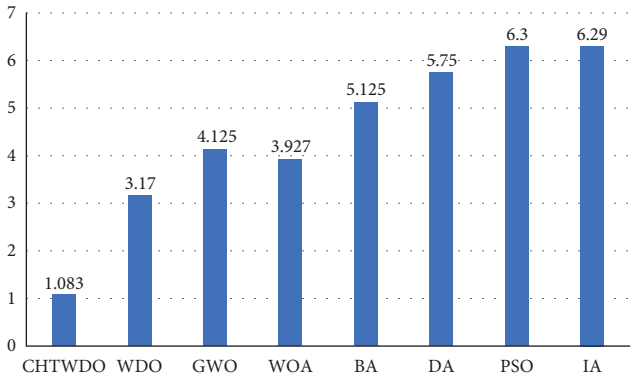


Figure 7: Friedman mean rank based on results in Table 2.

$$\tau(x) = \sqrt{(\tau')^2 + 2\tau'\tau''\frac{x_2}{R} + (\tau'')^2}, \tau' = \frac{P}{\sqrt{2}x_1x_2}, \tau'' = \frac{MR}{J},$$

$$M = P\left(L + \frac{x_2}{2}\right), R = \sqrt{\frac{x_2^2}{4} + \left(\frac{x_1 + x_3}{2}\right)^2},$$

$$J = 2\left\{\sqrt{2}x_1x_2\left[\frac{x_2^2}{4} + \left(\frac{x_1 + x_3}{2}\right)^2\right]\right\}, \sigma(x) = \frac{6PL}{x_4x_3^2}, \delta(x) = \frac{6PL^3}{Ex_4x_3^2},$$

$$P_C(x) = \frac{4.013\sqrt{\frac{x_3^2x_4^6}{36}}}{L^2}\left(1 - \frac{x_3}{2L}\sqrt{\frac{E}{4G}}\right),$$

$$P = 6000\,\text{lb}, L = 14\,\text{in}, \delta_{\max}\,\text{in}, E = 3 \times 10^6\,\text{psi},$$

$$G = 12 \times 10^6\,\text{psi}, \tau_{\max}\,\text{psi}, \sigma_{\max}\,\text{psi}.$$

All findings are compiled in Table 11 after 20 runs. All four indicators show the greatest results for CHTWDO. CHTWDO performs better on average value and STD, indicating that it is more stable, even if WDO also achieves the same data on best result. Table 12 shows the values of the variables for each algorithm's best outcome.

*5.2. Three-Bar Truss Design.* When constructing a truss with several constraints, such as deflection, buckling, and stress, the three-bar truss design aims to attain the least weight possible. This optimization issue contains two design parameters, $x1$ and $x2$, as illustrated in Figure 10. It is presented in mathematical form as follows:

Consider: $x = [x_1, x_2] = [A_1, A_2]$,

Minimize: $f(x) = (2\sqrt{2x_1} + x_2) \times l$,

Restriction condition:

$$\begin{cases} h_1(x) = \dfrac{\sqrt{2x_1} + x_2}{\sqrt{2x_1^2 + 2x_1x_2}}P - \sigma \le 0, \\ h_2(x) = \dfrac{x_2}{\sqrt{2x_1^2 + 2x_1x_2}}P - \sigma \le 0, \\ h_3(x) = \dfrac{1}{\sqrt{2x_1^2 + x_1}}P - \sigma \le 0, \end{cases} \tag{23}$$

Variables range: $0 \le x_1, x_2 \le 1$,

where $l = 100\,\text{cm}$, $P = 2\,\text{kN/cm}^2$, $\sigma = 2\,\text{kN/cm}^2$.

The best, mean, worst, and standard deviation of several algorithms used to solve the three-bar truss design

Table 7: Comparison of the average of WDO with a single improvement strategy.

| Algorithm | f1 | f2 | f3 | f4 | f5 | f6 | f7 | f8 |
|---|---|---|---|---|---|---|---|---|
| CHTWDO | **1.00E − 300** | **1.00E + 02** | **1.52E − 60** | **0** | **2.15E − 10** | **1.47E − 10** | **2.23E − 90** | **2.24E − 58** |
| CWDO | 3.69E − 175 | 1.08E + 02 | 3.47E − 34 | **0** | 3.65E − 06 | 6.17E − 05 | 8.04E − 68 | 1.08E − 42 |
| HTWDO | 8.49E − 258 | 1.03E + 02 | 1.07E − 45 | **0** | 5.72E − 09 | 2.42E − 08 | 1.48E − 84 | 8.94E − 56 |
| TWDO | 2.01E − 169 | 1.05E + 02 | 6.35E − 32 | **0** | 1.03E − 08 | 1.75E − 06 | 2.73E − 72 | 5.74E − 48 |
| | f9 | f10 | f11 | f12 | f13 | f14 | f15 | f16 |
| CHTWDO | **1.21E − 10** | **1.08E − 15** | **1.15E − 15** | **1.35E−15** | **8.08E − 13** | **−1.01E + 02** | **−1.02E + 01** | **3.30E − 04** |
| CWDO | 7.30E − 06 | 3.73E − 06 | **1.15E − 15** | 2.49E−10 | 3.41E − 07 | −7.89E + 01 | −1.39E + 01 | 3.88E − 04 |
| HTWDO | 1.78E − 10 | 4.02E − 12 | **1.15E − 15** | 7.42E−14 | 5.18E −12 | −6.43E + 02 | −1.16E + 00 | 3.41E − 04 |
| TWDO | 5.71E − 08 | 8.93E − 10 | **1.15E − 15** | 8.32E−12 | 2.39E − 10 | −2.51E + 01 | −9.91E + 00 | 3.79E − 04 |
| | f17 | f18 | f19 | f20 | f21 | f22 | f23 | f24 |
| CHTWDO | **7.96E − 01** | **−1.03E + 00** | **3.98E − 01** | **−3.86E + 00** | **−3.26E + 00** | **−1.02E + 01** | **−9.87E + 00** | **−9.87E + 00** |
| CWDO | 9.30E − 01 | **−1.03E + 00** | 4.65E − 01 | −2.38E + 00 | −2.49E − 07 | −1.36E + 00 | −1.39E + 00 | −3.88E + 00 |
| HTWDO | 8.18E − 01 | **−1.03E + 00** | 5.12E − 01 | −3.42E + 00 | −3.15E − 12 | −6.43E + 00 | −9.16E + 00 | −9.41E + 00 |
| TWDO | 8.54E − 01 | **−1.03E + 00** | 4.44E − 01 | −3.32E + 00 | −2.39E − 10 | −2.51E + 01 | −7.91E + 00 | −8.79E + 00 |

The significance of bold values represent the optimal values of each test function.

Table 8: Comparison of standard deviations of WDO with single improvement strategy.

| Algorithm | f1 | f2 | f3 | f4 | f5 | f6 | f7 | f8 |
|---|---|---|---|---|---|---|---|---|
| CHTWDO | **1.31E − 300** | **1.01E + 02** | **2.23E − 60** | **0** | **3.11E − 10** | **1.32E − 10** | **2.81E − 90** | **2.89E − 58** |
| CWDO | 5.03E − 175 | 2.38E + 02 | 5.48E − 34 | **0** | 7.65E − 06 | 8.47E − 07 | 7.15E − 49 | 3.27E − 46 |
| HTWDO | 7.84E − 258 | 1.03E + 02 | 1.27E − 50 | **0** | 8.92E − 09 | 1.96E − 09 | 1.64E − 86 | 1.92E − 56 |
| TWDO | 2.37E − 169 | 1.75E + 02 | 6.61E − 40 | **0** | 1.45E − 08 | 5.23E − 08 | 3.58E − 80 | 5.79E − 48 |
| | f9 | f10 | f11 | f12 | f13 | f14 | f15 | f16 |
| CHTWDO | **1.00E − 10** | **0** | **0** | **0** | **6.14E − 16** | **1.02E + 01** | **1.05E + 01** | **2.04E − 04** |
| CWDO | 4.32E − 08 | **0** | **0** | **0** | 5.39E − 07 | 6.19E + 01 | 4.79E + 01 | 3.58E − 04 |
| HTWDO | 1.62E − 10 | **0** | **0** | **0** | 4.53E − 14 | 1.40E + 01 | 7.86E + 00 | 4.03E − 04 |
| TWDO | 6.27E − 09 | **0** | **0** | **0** | 8.62E − 12 | 1.41E + 01 | 9.93E + 00 | 5.26E − 04 |
| | f17 | f18 | f19 | f20 | f21 | f22 | f23 | f24 |
| CHTWDO | **2.08E − 01** | **0** | **1.08E − 01** | **2.90E + 00** | **1.09E + 00** | **1.01E + 00** | **2.05E − 02** | **7.13E − 01** |
| CWDO | 4.17E − 01 | 1.08E − 04 | 1.90E − 01 | 8.31E + 00 | 5.62E + 01 | 6.32E + 01 | 1.69E − 01 | 3.58E − 00 |
| HTWDO | 3.62E − 01 | 7.38E − 06 | 1.26E − 01 | 6.04E + 00 | 4.13E + 00 | 2.17E + 01 | 3.46E − 01 | 9.94E − 01 |
| TWDO | 6.27E − 01 | 6.92E − 05 | 1.58E − 01 | 1.72E + 01 | 8.92E + 00 | 3.41E + 01 | 4.84E − 01 | 1.82E − 00 |

The significance of bold values represent the optimal values of each test function.

issue are shown in Table 13. CHTWDO continues to perform remarkably well and is the best algorithm overall. The determined optimal decision factors for the best solution for each comparison approach are listed in Table 14.

*5.3. Spring Design.* Wire diameter ($d$), the number of active coils ($N$), and mean coil diameter ($D$) are the three parameters for the spring system in this problem. The major objective of this topic is to determine how to optimize these factors to reduce the weight of the coil. The spring system is schematically shown in Figure 11, and the optimization model is provided by Equation (24).

Consider: $x = [x_1, x_2, x_3] = [d, D, N]$,

Minimize: $f(x) = (x_3 + 2)x_2x_1^2$,

Restriction condition:

$$\begin{cases} h_1(x) = 1 - \dfrac{x_2^3 x_3}{71785x_1^4} \le 0, \\ h_2(x) = \dfrac{4x_2^2 - x_1x_2}{12566(x_2x_1^3 - x_1^4)} + \dfrac{1}{5108x_1^2} \le 0, \\ h_3(x) = 1 - \dfrac{104.45x_1}{x_2^2x_3} \le 0, \\ h_4(x) = \dfrac{x_1 + x_2}{1.5} - 1 \le 0, \end{cases} \tag{24}$$

Variables range: $0.05 \le x_1 \le 2, 0.25 \le x_2 \le 1.30, 2.00 \le x_3 \le 15$.

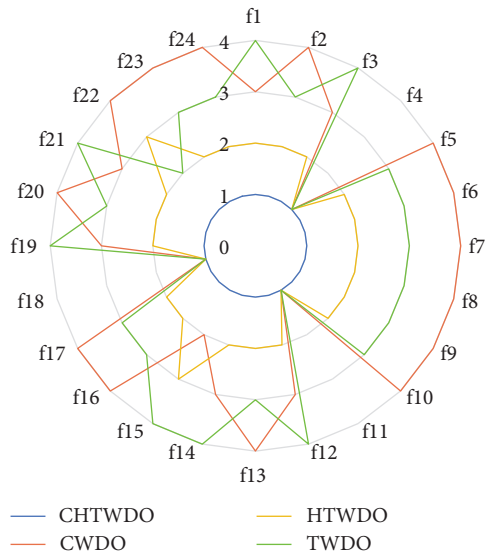


Figure 8: Radar map of WDO with single improvement strategy.

Table 9: Compared with the test results between CHTWDO and other scholars' improved WDO.

| Function | CHTWDO | | IWDO | | MFWDO | | GA-WDO | |
|---|---|---|---|---|---|---|---|---|
| | Average | Std | Average | Std | Average | Std | Average | Std |
| f1 | **1.00E − 300** | **1.31E − 300** | 1.64E − 175 | 3.72E − 175 | 9.68E − 258 | 8.13E − 258 | 7.32E − 169 | 2.67E − 160 |
| f2 | **1.00E + 02** | **1.01E + 02** | 1.21E + 02 | 4.61E + 02 | 1.22E + 02 | 2.86E + 02 | 1.37E + 02 | 4.92E + 02 |
| f3 | **1.52E − 60** | **2.23E − 60** | 3.42E − 57 | 1.48E − 54 | 6.30E − 49 | 5.82E − 48 | 7.65E − 32 | 6.88E − 30 |
| f4 | **0** | **0** | 6.32E − 190 | 7.70E − 190 | 1.81E − 178 | 9.22E − 176 | 4.84E − 164 | 6.05E − 160 |
| f5 | 2.15E − 10 | 3.11E − 10 | 3.65E − 08 | 5.51E − 06 | **5.72E − 11** | **3.08E − 10** | 1.03E − 09 | 9.25E − 09 |
| f6 | **1.47E − 10** | **1.32E − 10** | 9.85E − 08 | 1.38E − 07 | 4.55E − 08 | 2.49E − 08 | 7.30E − 09 | 8.91E − 09 |
| f7 | 2.23E − 90 | **2.81E − 90** | 8.74E − 88 | 6.23E − 87 | 8.58E − 90 | 6.46E − 90 | **9.21E − 92** | 7.78E − 90 |
| f8 | **2.24E − 58** | **2.89E− 58** | 1.37E − 46 | 7.01E − 45 | 9.36E − 56 | 5.87E − 54 | 5.26E − 49 | 6.82E − 50 |
| f9 | **1.21E − 10** | **1.00E − 10** | 8.27E − 07 | 5.24E − 08 | 6.22E − 10 | 1.74E − 10 | 4.96E − 09 | 9.54E − 09 |
| f10 | **1.08E − 15** | **0** | 6.19E − 09 | 4.18E − 09 | 8.50E − 12 | 2.15E − 12 | 3.58E − 14 | 1.69E − 14 |
| f11 | 1.15E − 15 | **0** | 9.53E − 15 | 8.47E − 14 | 1.45E − 15 | 9.66E − 15 | **1.02E − 15** | 6.95E − 14 |
| f12 | **1.35E − 15** | **0** | 4.89E − 12 | 2.67E − 12 | 1.71E − 14 | 6.82E − 14 | 8.49E − 13 | 5.26E − 13 |
| f13 | **8.08E − 13** | **6.14E − 16** | 3.62E − 09 | 2.16E − 09 | 8.49E − 12 | 8.73E − 12 | 6.75E − 12 | 5.65E − 12 |
| f14 | **−1.01E + 02** | **1.02E + 01** | −2.96E + 01 | 6.63E + 01 | −1.30E + 02 | 1.77E + 02 | −9.71E + 02 | 5.46E + 02 |
| f15 | **−1.02E + 01** | 1.05E + 01 | −9.40E + 01 | 5.73E + 01 | −7.16E + 00 | 7.55E + 00 | −9.21E + 00 | **2.71E + 00** |
| f16 | 3.30E − 04 | 2.04E − 04 | **2.20E − 04** | 9.26E − 04 | 2.26E − 04 | 3.78E − 04 | 2.35E − 04 | **1.23E − 04** |

The significance of bold values represent the optimal values of each test function.

Table 10: The results of the proposed methodology.

| Ratio | f1 | f2 | f3 | f4 | f5 | f6 | f7 | f8 | Geomean |
|---|---|---|---|---|---|---|---|---|---|
| CHTWDO | 5.32E − 01 | 1.35E + 00 | 1.79E + 00 | 7.18E − 01 | 1.21E + 00 | 9.99E − 01 | 1.09E + 00 | 1.47E + 00 | 6.93 E + 00 |
| WDO | 3.62E + 01 | 4.46E + 02 | 4.74E + 01 | 8.01E + 00 | 5.43E + 01 | 4.51E + 01 | 4.35E + 01 | 5.67E + 01 | 3.49E + 01 |
| | f9 | f10 | f11 | f12 | f13 | f14 | f15 | f16 | |
| CHTWDO | 6.65E − 01 | 2.90E + 00 | 2.91E + 00 | 4.95E − 01 | 3.98E + 00 | 5.72E − 01 | 3.31E + 00 | 1.11E + 00 | — |
| WDO | 5.15E + 01 | 9.83E + 00 | 9.32E + 01 | 9.55E + 00 | 2.51E + 01 | 9.79E + 00 | 3.58E + 01 | 5.23E + 01 | — |
| | f17 | f18 | f19 | f20 | f21 | f22 | f23 | f24 | |
| CHTWDO | 2.88E − 01 | 9.28E + 00 | 4.08E + 00 | 6.64E − 01 | 6.12E + 00 | 5.22E − 01 | 6.44E + 00 | 7.66E + 00 | — |
| WDO | 3.62E + 01 | 8.89E + 01 | 8.14E + 00 | 8.77E + 00 | 7.27E + 01 | 4.32E + 00 | 7.58E + 01 | 1.62E + 01 | — |

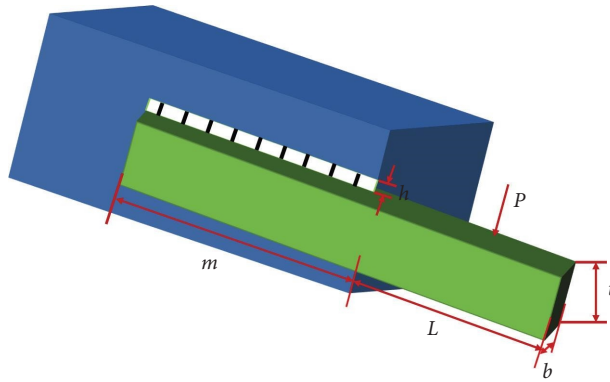


Figure 9: The welded beam design drawing map.

Table 11: Results of the welded beam design problem.

| Algorithms | Best | Mean | Worst | Std | Rank |
|---|---|---|---|---|---|
| CHTWDO | **1.724527** | 1.9142249 | 2.1056474 | 0.1175823 | **1** |
| WDO | **1.724527** | 2.0246610 | 2.2271271 | 0.2375921 | 2 |
| GWO | 1.724910 | 1.9528761 | 2.1444739 | 0.1802125 | 4 |
| WOA | 1.733462 | 2.6589611 | 3.1094312 | 0.7801672 | 7 |
| BA | 1.726240 | 1.9964298 | 2.8731091 | 0.5209634 | 5 |
| DA | 1.879950 | 2.1363578 | 2.9451802 | 0.4904327 | 8 |
| PSO | 1.729843 | 1.9275891 | 2.4980137 | 0.3089531 | 6 |
| IA | 1.724852 | 2.2614932 | 2.8091743 | 0.4308599 | 3 |

The significance of bold values represent the optimal values of each test function.

Table 12: The value of the variables when each algorithm obtains the optimal value in the welded beam problem.

| Algorithms | Optimal values for variables | | | | Optimum cost |
|---|---|---|---|---|---|
| | $h$ | $l$ | $t$ | $b$ | |
| CHTWDO | 0.187156 | 0.187156 | 0.187156 | 0.187156 | **1.724527** |
| WDO | 0.187156 | 0.187156 | 0.187156 | 0.187156 | **1.724527** |
| GWO | 0.203687 | 0.203687 | 0.203687 | 0.203687 | 1.724910 |
| WOA | 0.205700 | 0.205700 | 0.205700 | 0.205700 | 1.733462 |
| BA | 0.203137 | 0.203137 | 0.203137 | 0.203137 | 1.726240 |
| DA | 0.182129 | 0.182129 | 0.182129 | 0.182129 | 1.879950 |
| PSO | 0.204368 | 3.856979 | 3.856979 | 3.856979 | 1.719843 |
| IA | 0.205729 | 0.205729 | 0.205729 | 0.205729 | 1.724852 |

The significance of bold values represent the optimal values of each test function.

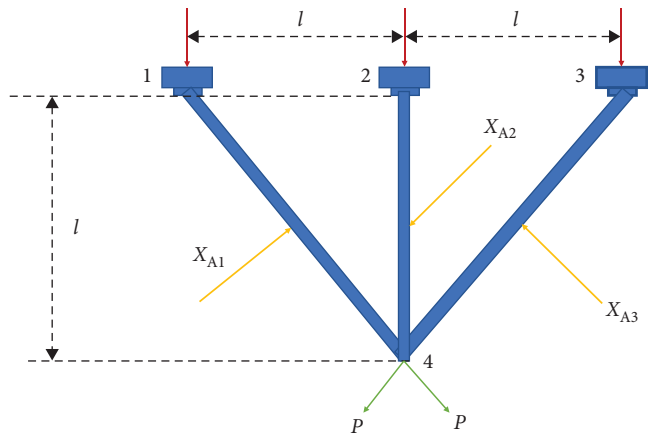


Figure 10: Schematic of the three-bar truss design.

Table 13: Results of the there-bar truss design problem.

| | Best | Mean | Worst | Std | Rank |
|---|---|---|---|---|---|
| CHTWDO | 291.7723 | 291.7877 | 291.7899 | 0.02849 | **1** |
| WDO | 303.5433 | 303.5451 | 303.5905 | 0.02964 | 8 |
| GWO | 292.1323 | 292.1392 | 292.1399 | 0.03027 | 3 |
| WOA | 292.2584 | 292.2797 | 292.2842 | 0.03351 | 4 |
| BA | 292.5509 | 292.5610 | 292.6141 | 0.12096 | 6 |
| DA | 292.1058 | 292.9142 | 293.0172 | 0.54818 | 2 |
| PSO | 292.4797 | 292.5026 | 292.8821 | 0.49729 | 5 |
| IA | 292.8279 | 292.8301 | 292.8491 | 0.39421 | 7 |

The significance of bold values represent the optimal values of each test function.

Table 14: The value of the variables when each algorithm obtains the optimal value in the three-bar truss design problem.

| | Optimal values for variables | | | | Optimum cost |
|---|---|---|---|---|---|
| | $h$ | $l$ | $t$ | $b$ | |
| CHTWDO | 0.187156 | 0.187156 | 0.187156 | 0.187156 | **1.724527** |
| WDO | 0.187156 | 0.187156 | 0.187156 | 0.187156 | **1.724527** |
| GWO | 0.203687 | 0.203687 | 0.203687 | 0.203687 | 1.724910 |
| WOA | 0.205700 | 0.205700 | 0.205700 | 0.205700 | 1.733462 |
| BA | 0.203137 | 0.203137 | 0.203137 | 0.203137 | 1.726240 |
| DA | 0.182129 | 0.182129 | 0.182129 | 0.182129 | 1.879950 |
| PSO | 0.204368 | 3.856979 | 3.856979 | 3.856979 | 1.719843 |
| IA | 0.205729 | 0.205729 | 0.205729 | 0.205729 | 1.724852 |

The significance of bold values represent the optimal values of each test function.

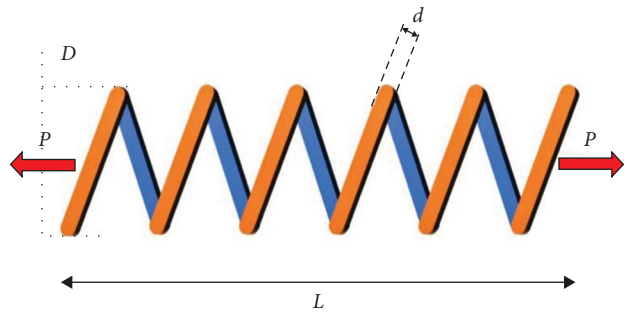


Figure 11: Schematic of the spring design problem.

Table 15: Results of the spring design problem.

| Algorithms | Best | Mean | Worst | Std | Rank |
|---|---|---|---|---|---|
| CHTWDO | **0.0127** | 0.0134 | 0.0142 | 0.0005 | **1** |
| WDO | 0.0130 | 0.0194 | 0.0203 | 0.0098 | 4 |
| GWO | 0.0130 | 0.0140 | 0.0161 | 0.0072 | 3 |
| WOA | **0.0127** | 0.0142 | 0.0198 | 0.0024 | 2 |
| BA | 0.0134 | 0.0153 | 0.0184 | 0.0016 | 5 |
| DA | 0.6408 | 0.7241 | 0.7803 | 0.2459 | 8 |
| PSO | 0.0598 | 0.0893 | 0.1035 | 0.0852 | 6 |
| IA | 0.0610 | 0.0704 | 0.0830 | 0.0281 | 7 |

The significance of bold values represent the optimal values of each test function.

Table 15 shows the final results produced by each program. Although WOA is comparable to CHTWDO in accuracy, it lags behind CHTWDO in mean and standard deviation. In this example, compared to CHTWDO, the results provided by the other algorithms are very inconsistent at runtime. However, CHTWDO maintains excellent robustness, which is critical in engineering applications. The ideal variables for this problem are shown in Table 16.

Table 16: The value of the variables when each algorithm obtains the optimal value in the spring design problem.

| | Optimal values for variables | | | Optimum cost |
|---|---|---|---|---|
| | $d$ | $D$ | $N$ | |
| CHTWMO | 0.0543 | 0.4316 | 7.9901 | **0.0127** |
| WMO | 0.0740 | 0.8482 | 4.8851 | 0.0130 |
| GWO | 0.0533 | 0.3960 | 9.5781 | 0.0130 |
| WOA | 0.0525 | 0.3775 | 10.168 | **0.0127** |
| BA | 0.0539 | 0.4025 | 9.4517 | 0.0134 |
| DA | 0.0623 | 0.6408 | 0.6408 | 0.6408 |
| PSO | 0.0598 | 0.0598 | 0.0598 | 0.0598 |
| IA | 0.0610 | 0.0610 | 0.0610 | 0.0610 |

The significance of bold values represent the optimal values of each test function.

## 6. Conclusions and Future Work

In this paper, a brand-new CHTWDO algorithm is suggested. First, using chaos theory, a more uniformly distributed beginning population is produced. To help choose the best search direction and start convergence to the optimum at the start of the search, the enhanced initial value can be seen from the convergence curve. The mining and exploration capacities are then improved using hyperbolic tangent and $T$-distribution, respectively. To evaluate the effectiveness of the enhanced algorithm, three different types of tests are planned. The E&P capabilities of CHTWDO were improved by the hyperbolic tangent and t distribution when compared to the original BWO and the single strategy BWO. In addition, 24 reference functions are chosen to compare seven conventional algorithms and seven innovative algorithms. In terms of solving accuracy, stability, and convergence speed, CHTWDO excels. For the purpose of evaluating the efficacy of this strategy in resolving real-world optimization issues, three traditional engineering examples are provided. CHTWDO came in first place among all engineering examples, demonstrating the algorithm's competitiveness in challenging search spaces. Future practical applications of the CHTWDO method could include path optimization, feature selection, parameter optimization, image processing, etc. The convergence process has improved the central deviation problem, but how to further reduce the proportion of central deviation needs further study.

## Data Availability

Data sharing is not applicable to this article as no data sets were generated or analyzed during the current study.

## Conflicts of Interest

The authors declare that there are no conflicts of interest in this paper.

## References

[1] L. Abualigah, A. Diabat, S. Mirjalili, M. Abd Elaziz, and A. H. Gandomi, "The arithmetic optimization algorithm," *Computer Methods in Applied Mechanics and Engineering*, vol. 376, Article ID 113609, 2021.

[2] H. Peraza-Vázquez, A. F. Peña-Delgado, G. Echavarría-Castillo, A. B. Morales-Cepeda, J. Velasco-Álvarez, and F. Ruiz-Perez, "A bio-inspired method for engineering design optimization inspired by dingoes hunting strategies," *Mathematical Problems in Engineering*, vol. 2021, Article ID 9107547, 19 pages, 2021.

[3] Y. Jia, S. Wang, L. Liang, Y. Wei, and Y. Wu, "A flower pollination optimization algorithm based on cosine cross-generation differential evolution," *Sensors*, vol. 23, no. 2, Article ID 606, 2023.

[4] A. Hassan, O. Bass, and M. A. S. Masoum, "An improved genetic algorithm based fractional open circuit voltage MPPT for solar PV systems," *Energy Reports*, vol. 9, pp. 1535–1548, 2023.

[5] M. Jaderyan and H. Khotanlou, "Virulence optimization algorithm," *Applied Soft Computing*, vol. 43, pp. 596–618, 2016.

[6] D. Li and L. Wang, "Optimization of township logistics distribution route based on simulated annealing algorithm," in *The Proceedings of the 5th International Conference on Energy Storage and Intelligent Vehicles (ICEIV 2022)*, F. Sun, Q. Yang, E. Dahlquist, and R. Xiong, Eds., Lecture Notes in Electrical Engineering, pp. 959–966, Springer, Singapore, 2023.

[7] V. Suthar, V. Vakharia, V. K. Patel, and M. Shah, "Detection of compound faults in ball bearings using multiscale-SinGAN, heat transfer search optimization, and extreme learning machine," *Machines*, vol. 11, no. 1, Article ID 29, 2023.

[8] M. Sun, Z. Cai, and H. Zhang, "A teaching-learning-based optimization with feedback for L-R fuzzy flexible assembly job shop scheduling problem with batch splitting," *Expert Systems with Applications*, vol. 224, Article ID 120043, 2023.

[9] H. Gao and M. Diao, "Cultural firework algorithm and its application for digital filters design," *International Journal of Modelling, Identification and Control*, vol. 14, no. 4, Article ID 324, 2011.

[10] D. Moldovan, I. Anghel, T. Cioara, and I. Salomie, "Adapted binary particle swarm optimization for efficient features selection in the case of imbalanced sensor data," *Applied Sciences*, vol. 10, no. 4, Article ID 1496, 2020.

[11] S. K. Dewi and D. M. Utama, "A new hybrid whale optimization algorithm for green vehicle routing problem," *Systems Science & Control Engineering*, vol. 9, no. 1, pp. 61–72, 2021.

[12] S. Mirjalili, A. H. Gandomi, S. Z. Mirjalili, S. Saremi, H. Faris, and S. M. Mirjalili, "Salp swarm algorithm: a bio-inspired optimizer for engineering design problems," *Advances in Engineering Software*, vol. 114, pp. 163–191, 2017.

[13] S. Bahuguna and A. Pal, "Robot path planning using $\beta$ hill climbing grey wolf optimizer," in *Proceedings of International*

*Joint Conference on Advances in Computational Intelligence*, M. S. Uddin, P. K. Jamwal, and J. C. Bansal, Eds., Algorithms for Intelligent Systems, pp. 295–304, Springer, Singapore, 2022.

[14] R. N. Khushaba, A. Al-Ani, A. AlSukker, and A. Al-Jumaily, "A combined ant colony and differential evolution feature selection algorithm, ant colony optimization and swarm intelligence," in *Ant Colony Optimization and Swarm Intelligence*, M. Dorigo, M. Birattari, C. Blum, M. Clerc, T. Stützle, and A. F. T. Winfield, Eds., Lecture Notes in Computer Science, pp. 1–12, Springer, Berlin, Heidelberg, 2008.

[15] T. K. Sharma and O. P. Verma, *Butterfly Optimization Algorithm: Theory and Engineering Applications*, Springer Nature, Singapore, 2022.

[16] G. Hu, B. Du, H. Li, and X. Wang, "Quadratic interpolation boosted black widow spider-inspired optimization algorithm with wavelet mutation," *Mathematics and Computers in Simulation*, vol. 200, pp. 428–467, 2022.

[17] M. A. Al-Betar, Z. A. A. Alyasseri, M. A. Awadallah, and I. Abu Doush, "Coronavirus herd immunity optimizer (CHIO)," *Neural Computing and Applications*, vol. 33, no. 10, pp. 5011–5042, 2021.

[18] D. Devassy, J. I. Johnraja, and G. J. L. Paulraj, "NBA: novel bio-inspired algorithm for energy optimization in WSN for IoT applications," *The Journal of Supercomputing*, vol. 78, no. 14, pp. 16118–16135, 2022.

[19] B. Das, V. Mukherjee, and D. Das, "Student psychology based optimization algorithm: a new population based optimization algorithm for solving optimization problems," *Advances in Engineering Software*, vol. 146, Article ID 102804, 2020.

[20] Z. Bayraktar, M. Komurcu, J. A. Bossard, and D. H. Werner, "The wind driven optimization technique and its application in electromagnetics," *IEEE Transactions on Antennas and Propagation*, vol. 61, no. 5, pp. 2745–2757, 2013.

[21] Z. Tang, S. Tao, K. Wang, B. Lu, Y. Todo, and S. Gao, "Chaotic wind driven optimization with fitness distance balance strategy," *International Journal of Computational Intelligence Systems*, vol. 15, no. 1, Article ID 46, 2022.

[22] I. Sokolik, "Introduction to the special issue "radiative transfer in the earth atmosphere," *Atmosphere*, vol. 12, no. 4, Article ID 479, 2021.

[23] J. Lin and H. Lin, "Introduction to the special issue on Earth's climate and weather: dominant variability and disastrous extremes," *Atmosphere-Ocean*, vol. 60, no. 3-4, pp. 141–148, 2022.

[24] W. Tang, J. Kang, L. Yang et al., "Thermosensitive nanocomposite components for combined photothermal–photodynamic therapy in liver cancer treatment," *Colloids and Surfaces B: Biointerfaces*, vol. 226, Article ID 113317, 2023.

[25] Z. Bayraktar, J. P. Turpin, and D. H. Werner, "Nature-inspired optimization of high-impedance metasurfaces with ultrasmall interwoven unit cells," *IEEE Antennas and Wireless Propagation Letters*, vol. 10, pp. 1563–1566, 2011.

[26] Z. Bayraktar, D. H. Werner, and P. L. Werner, "Miniature meander-line dipole antenna arrays, designed via an orthogonal-array-initialized hybrid particle-swarm optimizer," *IEEE Antennas and Propagation Magazine*, vol. 53, no. 3, pp. 42–59, 2011.

[27] A. Boulesnane and S. Meshoul, "A new multi-region modified wind driven optimization algorithm with collision avoidance for dynamic environments," in *Advances in Swarm Intelligence*, Y. Tan, Y. Shi, and C. A. C. Coello, Eds., Lecture Notes in Computer Science, pp. 412–421, Springer, Cham, 2014.

[28] Z. Bao, Y. Zhou, L. Li, and M. Ma, "A hybrid global optimization algorithm based on wind driven optimization and differential evolution," *Mathematical Problems in Engineering*, vol. 2015, Article ID 389630, 20 pages, 2015.

[29] Z. Bayraktar and M. Komurcu, "Adaptive wind driven optimization," in *Proceedings of the 9th EAI International Conference on Bio-Inspired Information and Communications Technologies (formerly BIONETICS)*, ACM, New York City, United States, 2016.

[30] Y. He, Y. Zhou, Y. Wei, Q. Luo, and W. Deng, "Wind driven butterfly optimization algorithm with hybrid mechanism avoiding natural enemies for global optimization and PID controller design," *Journal of Bionic Engineering*, vol. 20, no. 6, pp. 2935–2972, 2023.

[31] P. Di Barba, M. E. Mognaschi, S. Wiak, M. Przybylski, and B. Slusarek, "Wind-driven optimization for the design of switched reluctance motors," in *18th International Symposium on Electromagnetic Fields in Mechatronics, Electrical and Electronic Engineering (ISEF)*, pp. 1-2, IEEE, Lodz, Poland, September 2017.

[32] D. Mathew, C. Rani, M. R. Kumar, Y. Wang, R. Binns, and K. Busawon, "Wind-driven optimization technique for estimation of solar photovoltaic parameters," *IEEE Journal of Photovoltaics*, vol. 8, no. 1, pp. 248–256, 2017.

[33] I. A. Ibrahim, M. J. Hossain, B. C. Duck, and C. J. Fell, "An adaptive wind-driven optimization algorithm for extracting the parameters of a single-diode PV cell model," *IEEE Transactions on Sustainable Energy*, vol. 11, pp. 1054–1066, 2020.

[34] L. Abualigah, A. Diabat, and W. G. Zong, "A comprehensive survey of the harmony search algorithm in clustering applications," *Applied Sciences*, vol. 10, no. 11, Article ID 3827, 2020.

[35] D. H. Wolpert and W. G. Macready, "No free lunch theorems for optimization," *IEEE Transactions on Evolutionary Computation*, vol. 1, no. 1, pp. 68–82, 1997.

[36] F. K. Onay and S. B. Aydemir, "Chaotic hunger games search optimization algorithm for global optimization and engineering problems," *Mathematics and Computers in Simulation*, vol. 192, pp. 514–536, 2022.

[37] Y. Wang, Y. Xiao, Y. Guo, and J. Li, "Dynamic chaotic opposition-based learning-driven hybrid Aquila optimizer and artificial rabbits optimization algorithm: framework and applications," *Processes*, vol. 10, no. 12, Article ID 2703, 2022.

[38] C. Wan, B. He, Y. Fan, W. Tan, T. Qin, and J. Yang, "Improved black widow spider optimization algorithm integrating multiple strategies," *Entropy*, vol. 24, no. 11, Article ID 1640, 2022.

[39] G. J. McLachlan, R. W. Bean, and L. Ben-Tovim Jones, "Extension of the mixture of factor analyzers model to incorporate the multivariate *t*-distribution," *Computational Statistics & Data Analysis*, vol. 51, no. 11, pp. 5327–5338, 2007.

[40] X. Zhang and Z. Zhou, "Classifying colour differences in dyed fabrics using an improved hunger games search optimised random vector functional link," *Journal of Engineered Fibers and Fabrics*, vol. 17, 2022.

[41] P.-C. Chang, W.-H. Huang, C.-J. Ting, L.-C. Wu, and C.-M. Lai, "A hybrid genetic-immune algorithm with improved offsprings and elitist antigen for flow-shop scheduling problems," in *11th IEEE International Conference on High Performance*

*Computing and Communications*, pp. 591–596, IEEE, Seoul, Korea (South), June 2009.

[42] R. Wu, H. Huang, J. Wei et al., "An improved sparrow search algorithm based on quantum computations and multi-strategy enhancement," *Expert Systems with Applications*, vol. 215, Article ID 119421, 2023.

[43] J. Kudela, "The evolutionary computation methods no one should use," 2023, http://arxiv.org/abs/2301.01984.